Third Semi-Annual Progress Report

on

DYNAMICS AND CONTROL OF ESCAPE AND RESCUE FROM A TUMBLING SPACECRAFT

(1 June 1972 to 30 November 1972)

NASA Grant NGR 39-009-210

Principal Investigator

Marshall H. Kaplan

Associate Professor of Aerospace Engineering

The Pennsylvania State University

University Park, Pa. 16802

Submitted to:

National Aeronautics and Space Administration

Washington, D.C. 20546

December 1972

TABLE OF CONTENTS

Page

I. INTRODUCTION 1

II. PROGRESS TO DATE 2

III. FUTURE TASKS 4

IV. RENEWAL STATEMENT OF WORK. 5

APPENDICES

A. Despinning and Detumbling Satellites in Rescue Operations. 8

B. Moving Mass Schemes for Tumbling Stabilization 27

C. Optimization of Movable Mass Controls. 53

D. Flexibility Analyses and Simulations 62

I. INTRODUCTION

This third semi-annual status report on dynamics and control of escape and rescue from a tumbling spacecraft presents results and expectations based on 18 months of effort. Tasks outlined in the last progress report have been continued and bail-out analyses initiated. Accomplishments attained during the period from 1 June 1972 to 30 November 1972 are summarized in Section II and detailed discussions of appropriate topics appear in the appendices. Tasks to be carried out during the next six-month period are outlined in Section III.

Since the current grant will expire on 31 May 1973 and a great deal of related work remains to be done, a tentative statement of work for a renewal grant is included in Section IV. Results to date have been rewarding and have satisfied the original objectives of this project. Each new result has led to other technical questions of interest. It is proposed that both continued and new areas be studied in this follow-on grant.

Communication and dissemination of results is considered a primary part of university research. Thus, a summary of work to date was presented at the Fifth International Space Rescue Symposium, held at the 23rd Congress of the International Astronautical Federation, 8-13 October 1972, in Vienna, Austria. This paper, entitled, "Despinning and Detumbling Satellites in Rescue Operations," will appear in the proceedings of the symposium and is included here as

Appendix A. Substantial interest was shown in this paper by the attendees and other papers presented will be helpful to continue work on this grant.

The personnel situation on this project is unchanged except for the addition of one doctoral candidate who will be developing bail-out analyses. Two master's students and one doctoral candidate should be completing their work shortly. Each will write a thesis and appropriate publications.

II. PROGRESS TO DATE

Basic task assignments presented in the last progress report (June 1972) have not changed. The status of each topic is briefly discussed below.

Preliminary design of unmanned module for automatic dock and detumble (MADD) was previously presented and appears in Appendix A. Further analyses have been carried out. These include synthesis of a continuously throttable position control system and an initial design of an attitude control system. All propulsion units are assumed continuously throttable since the maneuvering requirements for this type of mission are extreme. A separate Astronautics Research Report will contain these analyses and simulations together with associated optimal detumble thrusting profiles. These profiles were based on constraining the magnitude of applied torque, and results indicate minimum time detumbling is obtained by always torquing along the negative angular momentum direction.

A movable mass control system to convert tumbling motion of a spacecraft into simple spin is being investigated. The equations of motion of a rigid spacecraft with attached control mass have been formulated. It is shown that a movable mass control system may increase the system energy to its maximum state,i.e., spin about the axis of minimum moment of inertia. It may also decrease the system energy to its minimum state, in which case spin would be about the axis of maximum inertia. The control system was designed for the latter case due to associated inherent stability and low spin rate. A control law relating control mass motions to vehicle motions was selected based on Lyapunov stability theory. For a selected spacecraft and realistic initial conditions, it is shown that the movable mass control system is capable of decreasing the kinetic energy of the system and establishing a simple spin state about the axis of maximum inertia within one hour. While this time may vary according to control system constraints, such as mass displacement amplitude or power, the feasibility of this system has been demonstrated. A comprehensive analysis and discussion of this control concept is included as Appendix B.

In addition to demonstrating feasibility of a moving mass system, optimization techniques are being employed to generate displacement profiles for the general problem of a tumbling asymmetrical body. Such techniques may permit rapid evaluation of these time histories for a large class of vehicle configurations. Methods are currently being refined to obtain solutions compatible with spacecraft constraints, A complete discussion of optimal control considerations appears in Appendix C.

Effects of long, flexible beams and solar arrays on the motion of a torque free, tumbling spacecraft are being investigated. Equations of motion are discussed for two asymmetrical vehicles with flexible beams and one spacecraft with two flexible solar arrays. Energy dissipation characteristics of the flexible appendages are investigated using the complex notation for structural damping. An assumed mode approach is used to describe the elastic deformations of these appendages. Initial conditions are such that only fundamental modes of vibration are considered. A comprehensive description of this treatment is offered in Appendix D.

A review of proposed "bail-out" procedures has been completed. Evaluation of these methods have determined those characteristics which allow reasonable safety and reliability. The departure angular motion of "bail-out" is determined by using Euler's equations for rigid bodies. Translational velocity depends on the point of departure with respect to the angular velocity vector. Methods of eliminating the undesirable motion of the astronauts have been investigated and two chosen as satisfying pertinent criteria. These are the Two Man Cable Despin device and the Extendable Rod Despin device.

III. FUTURE TASKS

Efforts will continue in the areas of moving mass optimization, flexibility effects on stabilization, and bail-out analyses. A separate Astronautics Research Report on the MADD concept and its

optimal detumbling capabilities will be completed during the next reporting period. A preliminary statement of work for a renewal grant beginning 1 June 1973 is included in the next Section.

Further work on the movable mass control system will be concerned with selection of sensors and determination of power requirements. Control system parameters must be selected such that the motion is within translation and power constraints, and optimal profiles are obtained. This effort will be coupling to an investigation of despinning methods to be used after stabilization by internal moving masses.

Flexibility analyses and simulations will be completed to the extent applicable to the current project objectives. The associated computer programs will be useful for estimating effects on the modular space station configuration. Devices for increasing dissipation rates through flexibility will also be suggested.

Simulations of bail-out dynamics will be performed through the use of a digital computer. These will aid in establishing procedures for leaving a tumbling vehicle such that a rescue craft can easily retrieve the crew. Optimum hatch locations and bail out timing should result.

IV. RENEWAL STATEMENT OF WORK

Activities on this grant have been confined to the analysis of tumbling, active detumbling technqiues, associated conceptual hardware, and operational aspects. It is proposed that current topics be continued and new areas be studied in a two-year renewal grant, as outlined below:

1. MADD Control Synthesis

Continuation of work to develop automatic control logic associated with tracking and docking during tumble. This will include simulations and animations of automated docking and detumble sequences.

2. Energy Dissipation Modeling

Continuation of work on dissipation modeling, including effects of fuel slosh and dampers. Work to date has been limited to flexibility effects.

3. Rescue Aids in Future Manned Spacecraft

Continued work on built-in devices to stabilize and aid in rescue operations will be performed. These include passive energy dissipators in addition to passive sensors for use by a rescue vehicle.

4. Escape Hatch and Bail-Out Analyses

Initial work on optimum placement of escape hatches has been done, but results will require further efforts. Simulations of various situations will be included to determine bail out dynamics and to evaluate individual detumble devices previously proposed.

5. Feasibility of Stick-On Rockets

A feasibility study of the stick-on rockets proposed by NAR is essential before further evaluation can be made. This would involve simulations of dynamics resulting from firing these rockets during tumble. The exact attachment points of these devices are critical to successful stabilization, In addition, the impulse imparted is also important.

6. Liquid Jet Experiments

Feasibility of using liquid jets for detumbling depends on a determination of jet properties in vacuum. Such properties are not known for conditions of interest in this situation. Facilities exist at Penn State for this kind of work and results can be obtained at a minimum of expenditure.

The principal investigator will participate on 1/4 time basis with other faculty contributing as needed. Three graduate assistants on 1/2 time schedules can handle the outlined tasks.

APPENDIX A

DESPINNING AND DETUMBLING SATELLITES IN RESCUE OPERATIONS*

by

Marshall H. Kaplan
Associate Professor of Aerospace Engineering
The Pennsylvania State University
University Park, Pennsylvania, U.S.A.

FIFTH SPACE RESCUE SYMPOSIUM
ORGANIZED BY THE SPACE RESCUE STUDIES COMMITTEE
INTERNATIONAL ACADEMY OF ASTRONAUTICS

Presented at the
23rd Congress of the International Astronautical Federation
8-13 October 1972
Vienna, Austria

---

*This work is supported by National Aeronautics and Space Administration Grant NGR 39-009-210.

I. INTRODUCTION

In the operation of future manned space vehicles there is always a finite probability that an accident will occur which results in uncontrolled tumbling of a spacecraft. The process of detumbling such a vehicle may represent a major part of the rescue operation if crewmen cannot evacuate while tumbling. Hard docking by a manned rescue craft is not possible because of complex maneuvers which would probably require excessive accelerations and fuel usage. In addition, the rescue crew would be exposed to an extremely hazardous environment since the tumbling vehicle may be larger than the rescue craft. Therefore, elimination of tumbling motion presents a very difficult problem which must be resolved to fulfill a complete space rescue capability.

The most general type of passive attitude motion is referred to as "tumbling." All three orthogonal components of angular velocity may be large, and there is no preferred axis of rotation. Since no spacecraft is absolutely rigid, tumbling motion will tend toward steady spin due to energy dissipation. However, large bodies such as manned space bases have relatively low dissipation rates and may require many days or weeks to passively stabilize at a constant spin rate about a single axis. If this state were reached, despinning is somewhat easier than detumbling. This paper discusses the operational aspects of detumbling or despinning a large passive vehicle during a rescue mission. Techniques and devices for carrying out these operations are also presented. Some specific examples are cited which represent realistic estimates of future rescue situations. Two philosophies are employed to consider promising methods of implementing attitude control; torque application from outside and built-in autonomous devices. The first category includes the use of fluid jets from a shuttle orbiter and a small automated thruster package to track and dock with the tumbling craft. Internal devices include self-contained, acceleration-activated mechanisms which may vary the

moments of inertia or apply thrust with time in order to stabilize motion to steady spin or eliminate all angular momentum.

II. THE NATURE OF TUMBLING

Angular momentum states have been classified according to motion and missions in which such states are likely to occur.[1] Simple spin is angular motion about a single body axis and is usually associated with passive attitude stabilization and the steady state of initially perturbed or tumbling bodies. Tumbling occurs immediately after a significant attitude perturbation, but eventually decays into simple spin. The nature of general torque-free tumbling motion of rigid bodies has been well established and may be described analytically or geometrically. For an unsymmetrical body the equations of motion are non-linear and cannot be solved without difficulty. A geometrical interpretation has been formulated by Poinsot.[2] The "Poinsot ellipsoid" illustrated in Figure 1 represents the locus of all possible values of angular velocity of the body which satisfy the constant kinetic energy condition. This imaginary ellipsoid is fixed to the body and moves with it, as shown. Attitude motion can then be described as the Poinsot ellipsoid rolling without slip on an inertially fixed plane with its center at a fixed distance from this plane. If the body is symmetric, the geometric interpretation is simpler and is illustrated in Figure 2. A "body cone" whose apex is at the center of mass and is fixed to the body rolls on an inertially fixed "space cone" whose axis coincides with the angular momentum vector. The common cone element coincides with the angular velocity vector.

Tumbling is the immediate result of a significant attitude perturbation to an uncontrolled vehicle with little or no initial spin. This situation is coupled with continuous angular motion of all three principal body axes, i.e., no inertially oriented axis exists. Crewmen trapped inside such a vehicle could not easily escape and may not even be able to move about due to the changing nature and magnitudes

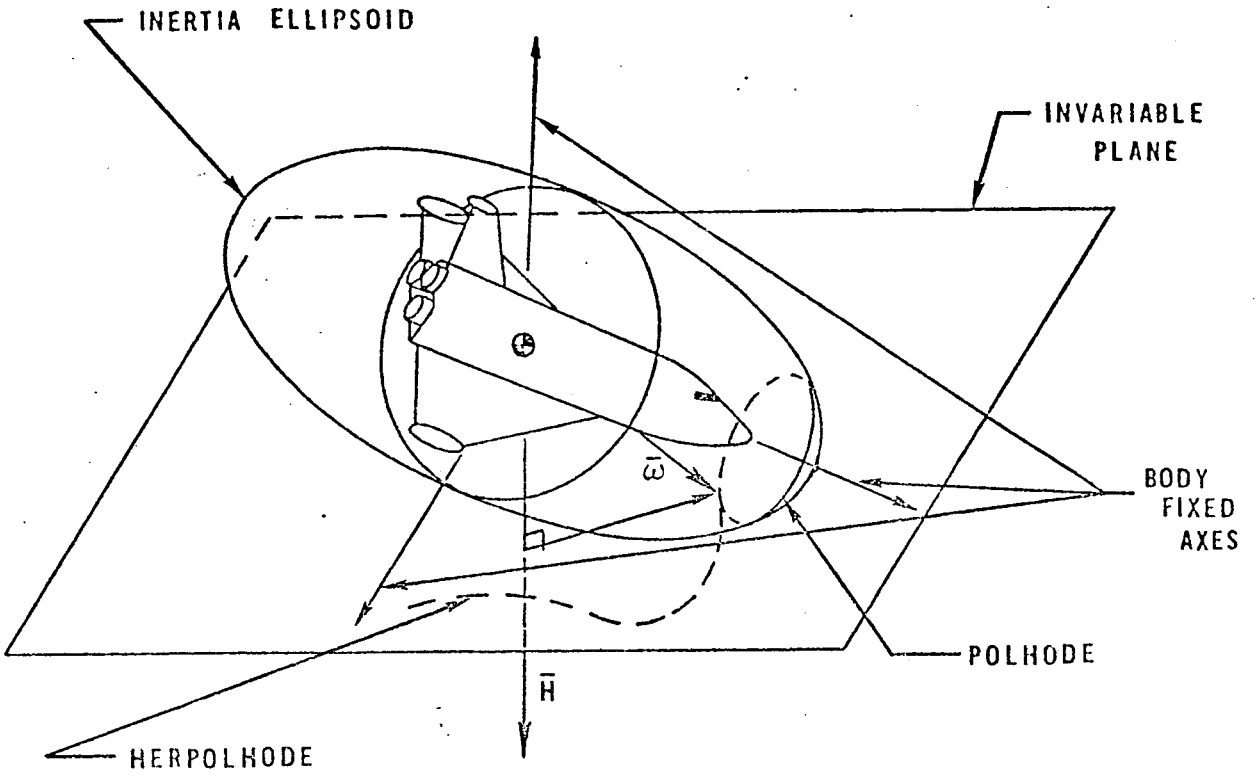

Figure 1. Geometric Interpretation of General Attitude Motion

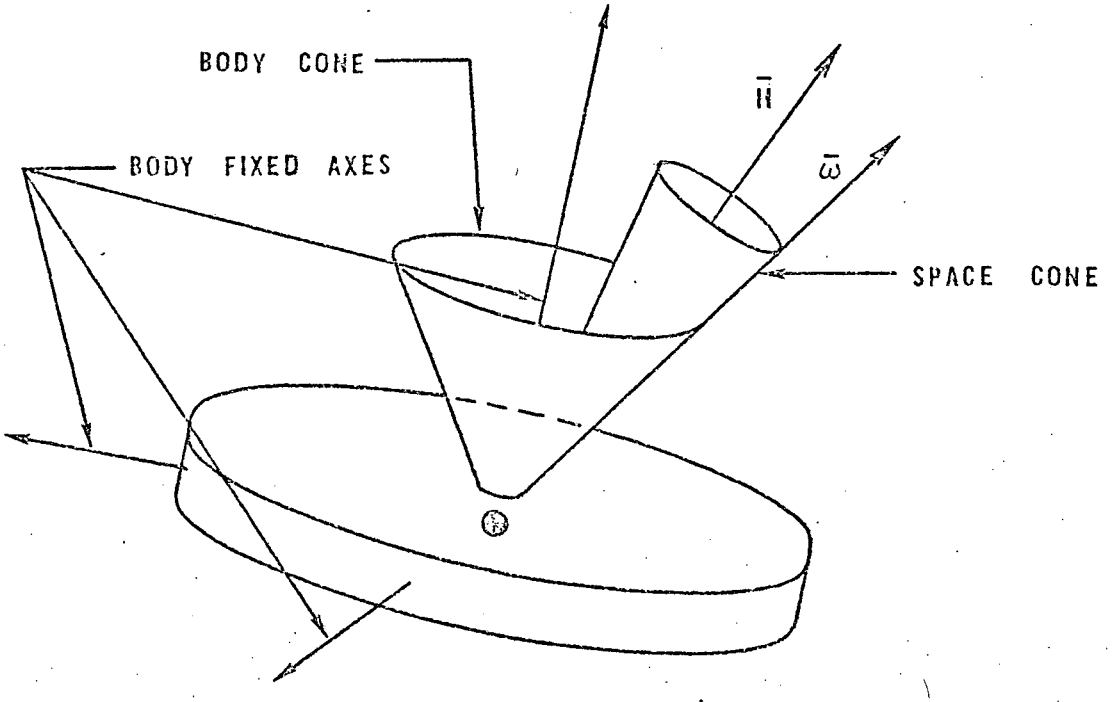

Figure 2. Geometric Interpretation of Axial Body Motion

of accelerations. This kind of attitude motion makes rescue very difficult. In general, elimination of angular motion of a large body is a complicated process, because it must be done either from a non-tumbling frame outside the body or by a possibly massive internal device which may only stabilize the motion to steady spin.

III. EXAMPLES OF TUMBLING SITUATIONS

In order to determine the requirements for a device or concept to detumble a large spacecraft some assumptions must be adopted about the causes of tumbling and calculations made to determine resulting maximum rates of tumble. An analysis of realistically determined situations was made with selected spacecraft which are thought to represent future mission hardware. Primary expected causes of tumbling associated with loss of control are vehicle-vehicle collisions, escaping atmosphere, pressure vessel rupture, runaway attitude thruster, and hard-over gimbal during a main engine firing.

Four configurations were selected based on a recent North American Rockwell study.[3] These are the modular space station, small space vehicle, Mark II orbiter, and generation 1 orbiter. Configurations are shown in Figure 3. Mass and moments of inertia were calculated for each vehicle and are listed in Table 1. Collisions between all combinations of these vehicles were considered, except Mark II-generation 1 orbiter encounters. Such mishaps were assumed to occur during docking operations with a relative velocity of 1.5m/sec with misalignment of 4 deg in angle and 0.61m in displacement in addition to an angular vehicle rotation rate of 0.1 deg/sec. Impact parameter values were assumed and energy methods of analysis were used to determine resulting tumbling rates. The escaping atmosphere situation was assumed for the modular space station and small space vehicle. Pressure wall perforation could result from meteorite penetration, internal explosion, etc. The effect on attitude is similar to that of a reaction jet as the inside atmosphere escapes into space. Worst cases were assumed with respect to

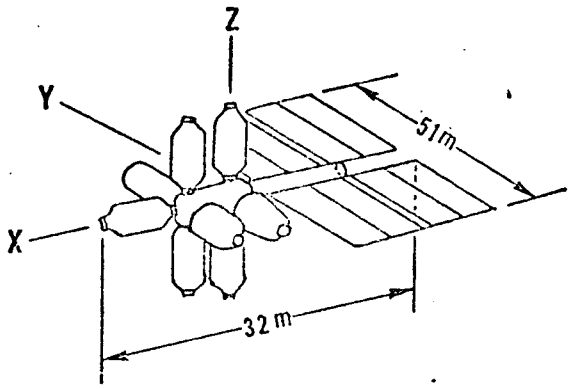

Modular Space Station

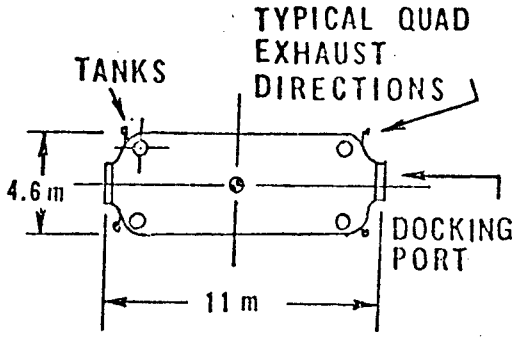

Small Space Vehicle

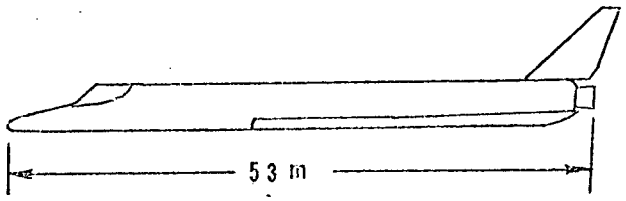

Mark II Orbiter

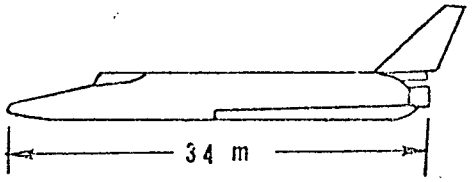

Generation 1 Orbiter

Figure 3. Configurations Considered in Tumbling Analysis

puncture location and thrust produced. Escape of fluids from tanks into space will have similar results to those of an escaping atmosphere. A single tank was assumed ruptured for each configuration studied. Worst case conditions prevailed, e.g., contents escaped in one direction producing thrust with a large moment arm about the center of mass.

Since only the two orbiter configurations have steerable main rockets, the hard over gimbal situation applied to them exclusively. Two thrusters on each vehicle were assumed fixed at maximum gimbal angle and fired for 15 sec. The final tumble-producing situation is concerned with a malfunctioning attitude thruster which is assumed to thrust for one minute.

Table 1 Mass Properties of Configurations Considered

		Modular Space Station	Small Space Vehicle	Mark II Orbiter	Generation 1 Orbiter
Mass (Kg)		100,000	11,400	138,000	81,000
Moments of Inertia ($Kg-m^2$)	I_{XX}	0.636×10^7	0.298×10^5	3.4×10^6	0.993×10^6
	I_{YY}	0.664×10^7	1.34×10^5	24.8×10^6	8.14×10^6
	I_{ZZ}	0.515×10^7	1.34×10^5	28.3×10^6	8.50×10^6
Products of Inertia ($Kg-m^2$)	I_{XY}	0.19×10^6	0	-1.22×10^4	0
	I_{XZ}	0.785×10^4	0	3.59×10^5	0
	I_{YZ}	0.176×10^4	0	0.271×10^4	0

Results of worst case situations are summarized in Table 2. It must be stressed that the values of angular rates appearing in this Table represent only the initial motion at the end of application of perturbing torque. Since the X, Y, and Z axes do not generally coincide with the principal body axes (motion about the maximum and minimum principal axes is stable for a rigid body) these spin modes will become tumbling modes within a few revolutions of the vehicle. Some of the results are given as ranges of angular rates because of parameter uncertainties in the analysis. In general, one could conclude that angular rates could be expected up to about 9.0 RPM for the large vehicles and up to about 14.7 RPM for the small space vehicle. The escaping atmosphere situation for this last vehicle is considered a catastrophic one, because a spin rate of 52 RPM would probably result in massive structural failure. Therefore, rescue from this spacecraft would be neither possible nor necessary. A few cases could not be analyzed due to a lack of data on configuration dimensions and layout details. However, all cases in which rescue is possible appear to be limited to initial angular rates of less than 10 RPM or 60 deg/sec for large vehicles and less than 15 RPM or 90 deg/sec for the small vehicle.

IV. RESCUE OPERATIONS

In general orbital rescue missions may be divided into three phases:[4] rescue alert and rendezvous with the disabled vehicle, rescue operations proper, and return of the rescue vehicle. The second phase is of primary concern here, since a major part of this phase involves detumbling a large, manned vehicle before evacuation and repairs can take place. The sequence of rescue operations depends on the type of control to be used. Two techniques are being considered: application of controlling torques from outside and stabilization by autonomous internal devices.

External application of torque can be done by either a programmed fluid jet or thruster package which maneuvers and docks with the

Table 2 Summary of Maximum Initial Tumbling Rates

	Modular Space Station	Small Space Vehicle	Mark II Orbiter	Generation 1 Orbiter
Collisons	ω_X=0.6-2.1RPM	ω_Y=4.7-14.7RPM ω_Z=4.7-14.7RPM	ω_Y=0.3-1.09RPM	ω_Y=0.5-1.45RPM
Escaping Atmosphere	ω_Z=8.9RPM	ω_Y=52RPM ω_Z=52RPM	I.D.	I.D.
Escaping Fluids	0.4-4.0RPM	I.D.	I.D.	I.D.
Hard Over Gimbal	Does Not Apply	Does Not Apply	1 - 2RPM	1 - 2RPM
Malfunctioning Thruster	.03RPM	ω_Y=0.5-4.0RPM	0.5-4.0RPM	I.D.

I.D. = INSUFFICIENT DATA TO ANALYZE

disabled vehicle if tumble rates are not too high. Operationally the rescue craft "parks" at an optimal position with respect to the tumbling vehicle. If a fluid jet is used the jet must impinge the structure such that angular momentum is decreased. This requires careful aiming and variation of jet intensity with time. Improper application could increase tumbling and cause structural damage. If an automated detumbling package is used it must maneuver to an anticipated rendezvous point on the disabled vehicle and then track the intended docking position while maneuvering in to make a "hard-dock." After this is accomplished, thrusters on this device apply a sequence of torques to the vehicle. This may be done optimally to use a minimum of fuel or time to detumble the craft.

Before application of torque or initiation of maneuvering to dock, it is necessary to determine the components of tumbling and angular momentum. Since the disabled vehicle is passive (assuming no autonomous devices were placed in this spacecraft for the specific purpose of measuring angular rates and/or stabilizing the vehicle) this determination must be done from the rescue craft. Such measurements are difficult to make, because angular components vary continuously with time in the general case. Three components of angular velocity are required simultaneous to obtain the direction and magnitude of angular momentum if the vehicle moments of inertia are known. Otherwise, extensive measurements are required. This latter situation is very likely to be the case if an explosion or loss of propellant has taken place. Techniques which employ visual observations, radar scanning, and laser reflectors in conjunction with onboard computers are likely candidates for these measurements. Special passive reflectors may be required on the disabled vehicle, but these are small, simple devices which can be mounted before launching all manned vehicles.

V. AUTOMATED EXTERNAL DETUMBLING DEVICES

Since the expected tumbling rates for large vehicles are relatively low, a small maneuverable thruster package deployed from the rescue craft could rendezvous and dock with the disabled vehicle while tumbling. A Module for Automatic Dock and Detumble (MADD) could perform an orbital transfer from the shuttle in order to track and dock at a preselected point on the distressed craft. Once docked MADD could apply torques by firing its thrusters to detumble the passive vehicle. This could be done in a minimum time or fuel sequence.

Design of a MADD type spacecraft is influenced by mission objectives and systems constraints. It must maneuver to, dock with, and detumble a large vehicle with limited fuel, and it must be adaptable to varying situations. Size is constrained by cargo bay dimensions of the rescue craft and to some extent geometry of the disabled vehicle. A preliminary configuration for MADD is shown in Figure 4. This version is designed to use an existing docking port on the disabled vehicle, although, there are some situations in which this is not possible or desirable. Other types of attachment devices may be adapted for those cases. All subsystems are contained within the octagonal structure and include control electronics, attitude control gyros, command and telemetry, propulsion, power, and various sensors.

The control system has three basic operating modes: transfer, dock, and detumble. During transfer from the rescue craft this system maintains attitude and reorients MADD just before entering the docking mode in which tumble tracking and attachment take place. As soon as hard docking is accomplished the detumble mode is initiated. During this last phase gyro controllers are locked and rate gyros are used for attitude reference. A single propulsion system will satisfy the requirements for transfer, detumble, and momentum dumping. Thrust profiles during tracking and detumbling phases are computed by an on-board computer based on measurements from sensors and those taken immediately upon completion of docking. Optimal sequences are

generated in order to detumble in minimum time with limited thrust when time is a critical factor.

The operational procedure for the use of MADD consists of deploying the module, transfer to a rendezvous point, tracking a docking port, hard docking, and detumbling. Before initiating this sequence, the rescue craft crew must determine the angular momentum and physical state of the disabled vehicle. An optimum parking position is selected for the rescue craft based on visual observation advantage, propellant requirements for maintaining this position, and possible transfer paths for MADD. Figure 5 shows a situation requiring a minimum propellant requirement for the rescue craft. Both vehicles share the same orbit but remain separated along the flight path. Once a stand-off situation is established, MADD is deployed from the cargo bay and the transfer phase begins. A general transfer profile is illustrated in Figure 6. Direct observation of MADD is possible from the rescue craft during the transfer phase. However, during tracking and docking radio and visual contact may be lost intermittently due to occultation. The rendezvous point can be selected such that the velocity of MADD at this point will coincide with the velocity of the disabled vehicle reference point. This will eliminate the need for a terminal maneuver by MADD before the tracking phase begins. The rendezvous point should typically be about 3 meters from the docking port. MADD thrusters begin firing to maintain and then reduce its distance to this port. Passive docking aids may be required around the port for sensing relative position, orientation, and velocity. This permits proper alignment during closure and docking. The process is continued until capture latches are secured. After detumbling crew evacuation takes place.

VI. AUTONOMOUS INTERNAL CONTROL MECHANISMS

Although detumbling by external means is a more positive technique and requires little of the disabled vehicle, it may be desirable to have internal devices which could at least lessen the tumbling motion

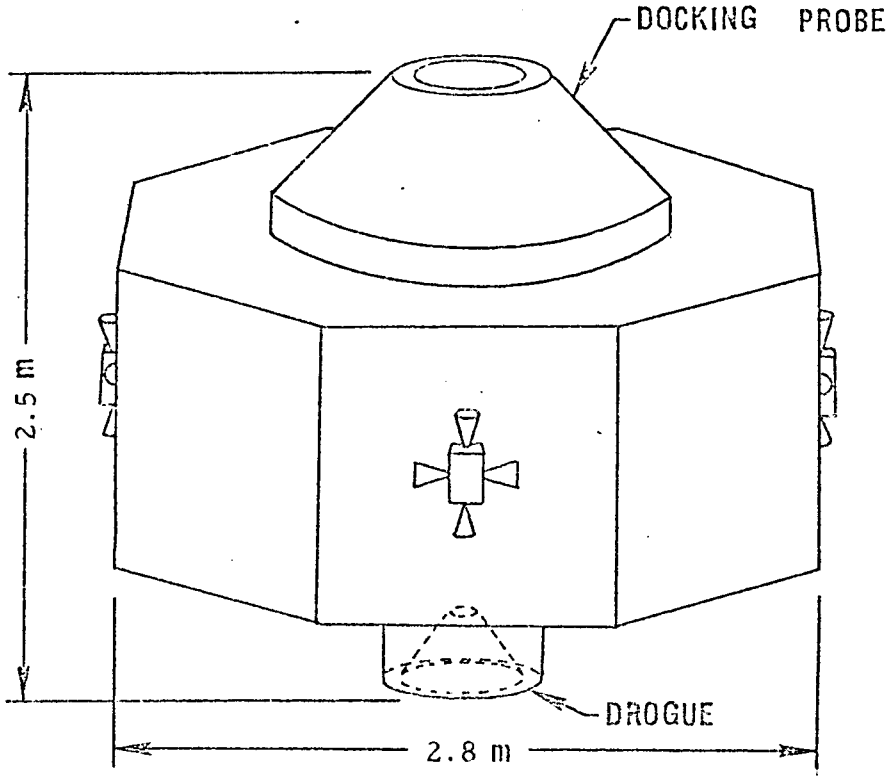

Figure 4. Preliminary Design for MADD

before a rescue craft arrives. Such devices would become effective upon loss of control and some could be relatively simple and lightweight.

Devices for controlling tumbling may be active or passive. Active devices use sensing instruments of some sort to command control torques. These systems require control logic and power. Typical mechanisms of this type are mass expulsion and momentum exchange devices. Another potential active control mechanism is a moveable mass system. By varying the position of a control mass properly, (i.e., changing the moments of inertia of the spacecraft) tumbling may be transformed into spin. Typical passive devices use the "wobbling" motion of the vehicle to activate simple mechanical or fluid devices which dissipate energy and lead to a simple spin state. Possible passive mechanisms include viscous ring and pendulum dampers.

Mass expulsion systems for use as internal detumbling devices may be of monopropellant or bipropellant type. The monopropellant type appears to be more desirable since bipropellant systems tend to be heavier and more complex. The simplest means of orienting the thrusters is to place pairs about each control axis. However, due to weight limitations this may not be possible, in which case it would be necessary to determine the number of thrusters needed and the best placement of these thrusters. Two drawbacks of mass expulsion devices are that they are massive and require an onboard power supply. For long term storage they may have questionable reliability.

Momentum-exchange devices have found many applications in the attitude control of satellites. The control scheme for momentum exchange devices is to store the unwanted tumbling motions of the spacecraft in the motions of a wheel. The moveable mass system for control of tumbling has been suggested for a number of applications. The concept is based on the assumption that the components of the spacecraft can move relative to each other. In the simplest case a control mass would move relative to the spacecraft in such a way that

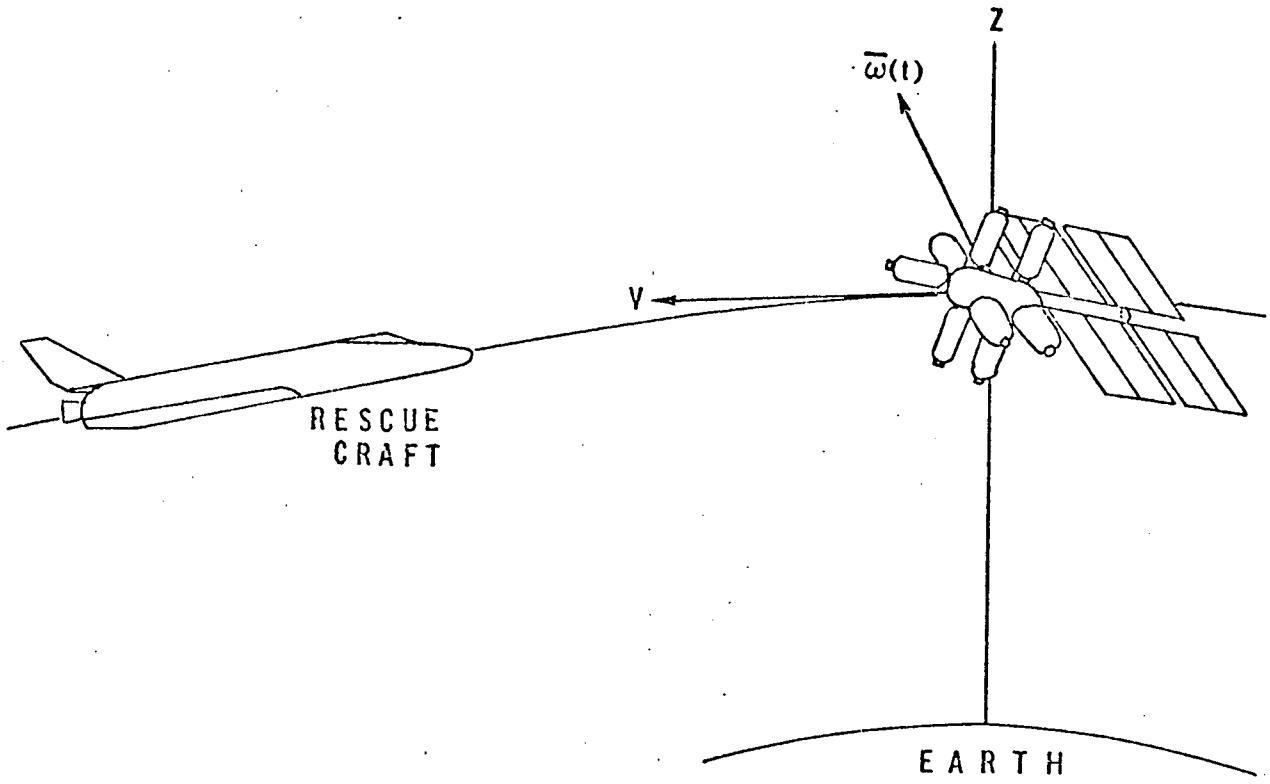

Figure 5. Example of Stand-Off Situation

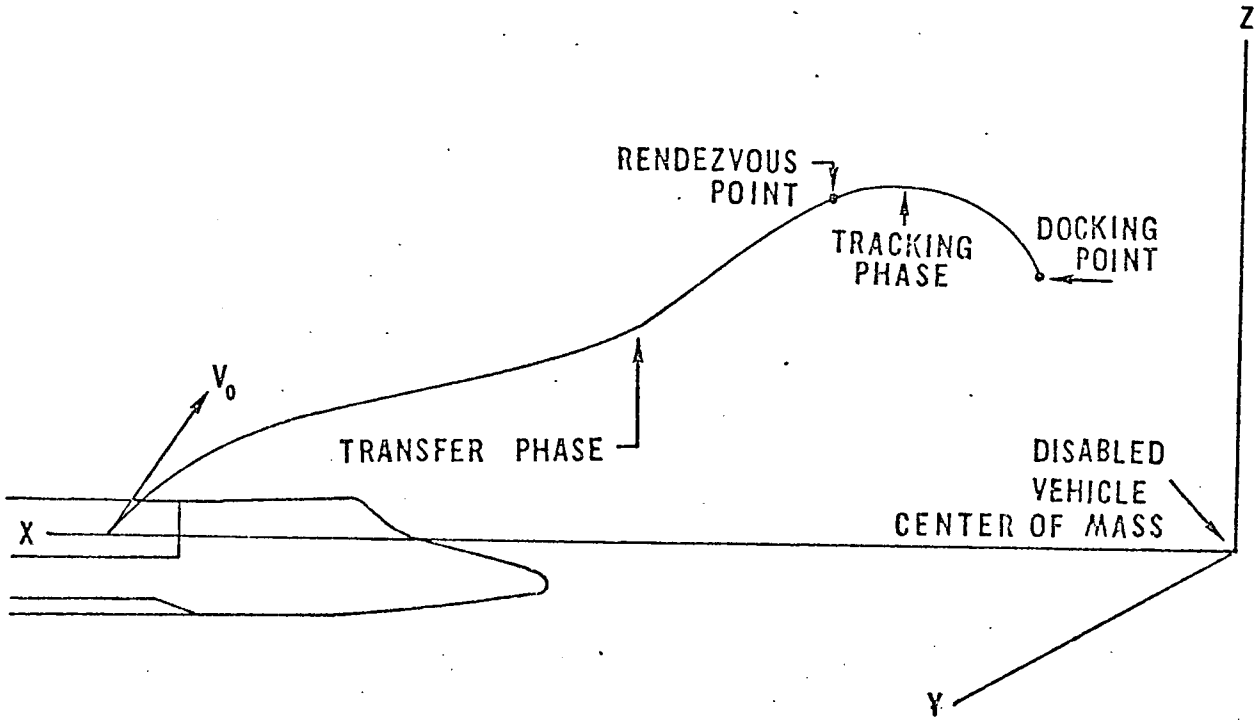

Figure 6. Typical Transfer Trajectory for MADD

kinetic energy decreases to a minimum at which time the spacecraft will be in a stable spin state. Once this state has been reached the spacecraft may be despun with another internal device or by external techniques. A simple spin state might also greatly facilitate crew escape.

VII. OPTIMAL DETUMBLING STRATEGY

The minimum time optimal detumbling of a distressed space vehicle can be divided into the following categories: constraint on the magnitude of the control moment vector and constraint on the magnitude of each component of this vector. The general problem of detumbling considered here is to bring all three components of angular velocity to zero in minimum time. The first constraint category can be handled with relative ease. The appropriate analysis was applied to an example case. A collision between a modular space station and a Mark II orbiter was assumed with a resulting tumble of the space station. Principal axis angular velocity components at commencement of external thrust application by MADD were taken as 1.150, 1.750 and -0.445 RPM about the 1, 2 and 3 principal axes, respectively. These values represent a good test situation for the optimization technique used. These components were brought to zero in about 7 minutes with a control torque magnitude of 3,390 N-m. Figure 7 shows a time history of the principal axis angular velocities during application of the optimum control moment. Figure 8 gives a time history of the body fixed thrusts required at point X = 3.9m, Y = 0.89m and Z = 18.3m to give the necessary 3,390 N-m moment directed opposite to the angular momentum vector.

The second type of constraint presents more difficulty in determining the optimum minimum time control moment sequence. In this case, the analysis is not as easily accomplished, and the control moment vector is not simply directed opposite to the angular momentum vector.

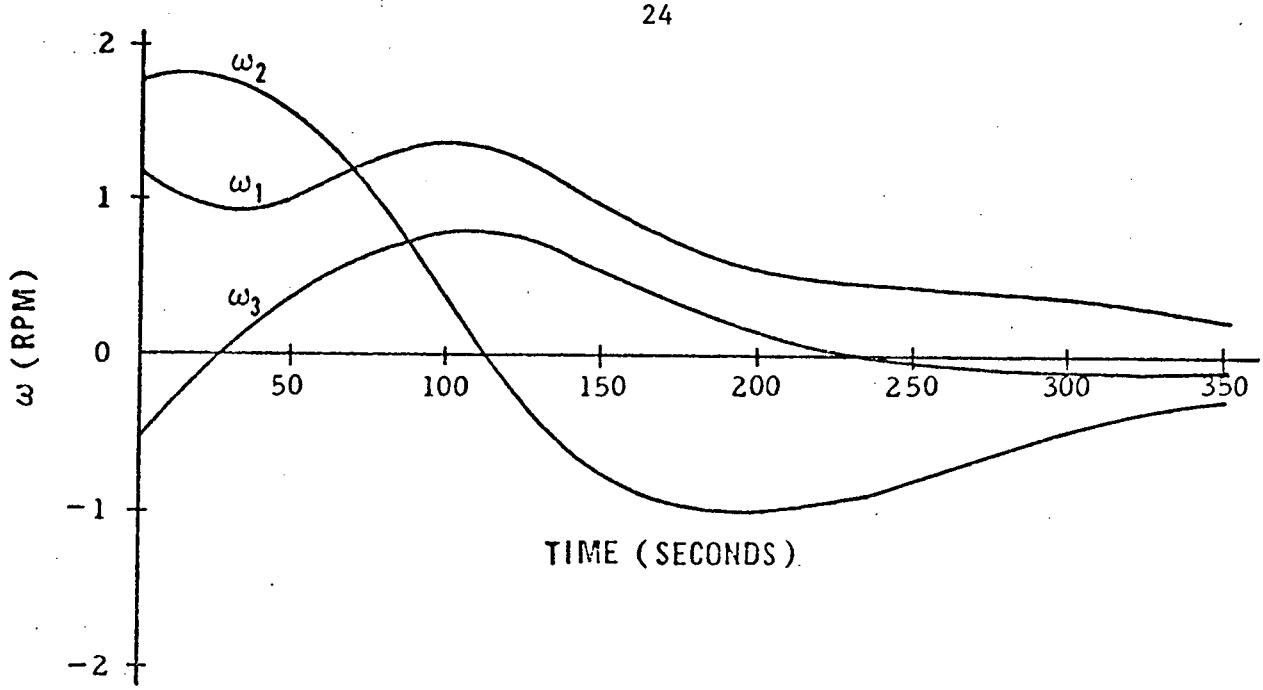

Figure 7. Principal Angular Velocities During Detumbling

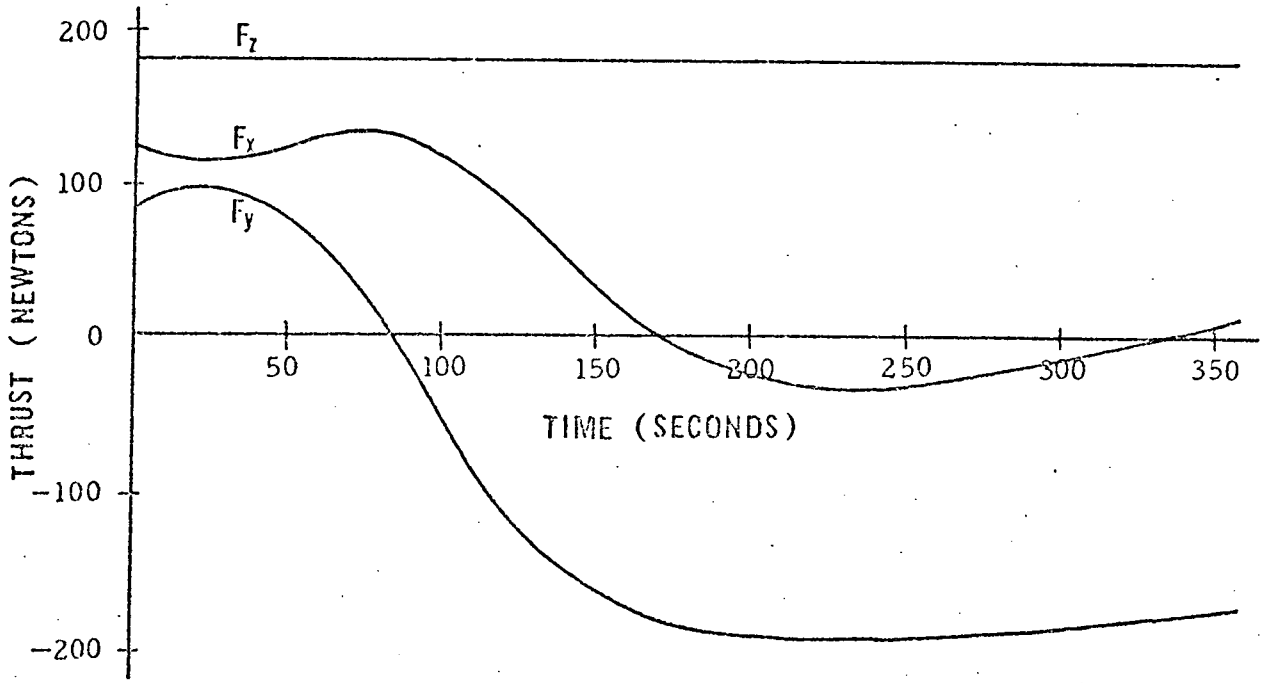

Figure 8. Body Fixed Thrust Component Profiles During Detumbling

VIII. CONCLUSIONS AND RECOMMENDATIONS

A rescue situation involving an uncontrolled, tumbling spacecraft is a definite possibility and one which requires special techniques and equipment. Such cases may require the elimination of tumble before evacuation of crewmen. The two basic approaches to the control of tumbling are concerned with external torque application and internal autonomous mechanisms. Several conclusions can be drawn from this study. These are listed below and refer to future manned spacecraft designs:

1) Reflectors designed for tumble state determination should be placed strategically about the outside of each vehicle.
2) Each new spacecraft design should be examined for possible inclusion of moving mass and/or passive dissipative devices.
3) Passive sensors for MADD docking alignment should be installed around all docking ports.
4) Realistic tumble rates are expected to be low, permitting the use of small thruster modules such as MADD.
5) Internal autonomous devices are desirable but cannot be expected to completely detumble the vehicle unless they are massive. Thus, outside torque application should be anticipated for future rescue missions.

Several recommendations are associated with these conclusions and refer to new technology areas:

1) Development of MADD units should be considered in depth. New technology will be required for at least the automatic control system and sensors.
2) Hardware components should be developed for use in determining tumbling rates through outside observations.
3) An extensive investigation of the properties of fluid jets into vacuum should be made to determine feasibility and application with respect to applying detumbling torques.
4) Simple and lightweight mechanisms should be sought for use as internal controlling elements to aid in detumbling.

Control concepts for MADD and new internal autonomous mechanisms are being investigated in the current study. New technology needed to make appropriate decisions regarding future space rescue capabilities is the primary objective of this program.

REFERENCES FOR APPENDIX A

1. Kaplan, M. H., "The Problem of Docking with a Passive Orbiting Object Which Possesses Angular Momentum," presented at the 22nd Congress of the International Astronautical Federation, Brussels, September 1971.
2. Thomson, W. T., Introduction to Space Dynamics, Wiley and Sons, 1963, pp. 113-130.
3. "Analysis of Tumbling Spacecraft," Final Report, Safety in Earth Orbit Study, Vol. III, North American Rockwell, Report No. SD 72-SA-0094-3, June 1972.
4. Wild, J. W. and Schaefer, H., "Space Rescue Operations," presented at the 3rd International Symposium on Space Rescue at the 21st Congress of the International Astronautical Federation, Constance, Germany, October 1970.

APPENDIX B

MOVING MASS SCHEMES FOR TUMBLING STABILIZATION

I. INTRODUCTION

Internal autonomous control devices for detumbling a space vehicle can be broadly classified as active or passive. Passive devices use the "wobbling" motions of the tumbling vehicle to activate simple mechanical or fluid devices which dissipate energy and lead to a simple spin about the maximum moment of inertia axis. Several types of these devices, such as the viscous ring and pendulum dampers, have been discussed in the literature. However, these devices are most appropriate for vehicles which have a high nominal spin rate about one axis. Active devices utilize sensors to command control torques to effect detumbling. Two examples of active control devices are mass expulsion and momentum exchange control systems. Mass expulsion systems require onboard storage of propellant and may not be reliable on a long term basis. Some momentum exchange devices may require continuous operation since startup would be difficult once a tumbling situation has occurred. These devices also have a tendency for saturation in large corrective maneuvers. One attractive tumbling stabilization device is the movable mass control system. This device moves a control mass, according to a selected control law, in the force field created by the tumbling motions. By moving the mass properly, the kinetic energy of the system may be increased or decreased creating

simple spin states about the minimum or maximum axes of inertia, respectively. This would greatly facilitate crew escape or final despinning by another means.

The treatment of moving masses inside a rigid main body has been treated descriptively by Grubin[1] and Roberson.[2] Grubin developed the equations of motion with respect to the main body center of mass while Roberson developed them with respect to the composite center of mass of the system. Kane and Scher[3] suggest using the effect of a movable mass to control a tumbling vehicle. Childs[4] has designed a movable mass control system for use in a space station which operates in an artificial -g mode. However, this control system is designed to damp out only small transverse tumble rates. Lorell and Lange[5] have developed an automatic mass-trim system to counteract sensor-vehicle misalignments. However, this analysis, and most reports on the subject, make the assumption of either small transverse tumble rates which permit linearization or assume a symmetric vehicle. These assumptions negate their validity for the general case of an asymmetric vehicle with arbitrary tumble rates.

It is the purpose of this report to develop the equations of motion of an asymmetric vehicle with attached movable mass and develop a control law which is applicable for arbitrary tumbling motions. A control law is selected and an example case is presented to demonstrate the feasibility of a movable mass control system to convert the tumbling motions of a vehicle into simple spin.

II. EQUATIONS OF MOTION

The equations of motion of a rigid spacecraft with an attached movable mass are developed in this section. In the following analysis $\frac{d}{dt}\vec{v}$ implies differentiation with respect to an inertial reference frame and $[\dot{\vec{v}}]$ implies differentiation with respect to the body fixed reference frame.

The generalized angular momentum equation for a rigid body with n moving masses is[1]

$$\vec{M} = \frac{d}{dt}\vec{H} + \vec{S} \times \vec{a} \tag{1}$$

where $\vec{M}$ is the external moment, $\vec{H}$ is the angular momentum of the system, $\vec{S}$ is the first moment of mass of the system, all with respect to an arbitrary reference point moving in an arbitrary manner, and $\vec{a}$ is the inertial acceleration of the reference point. Equation (1) reduces to the standard equation $\vec{M} = \frac{d}{dt}\vec{H}$ for the usual cases where the reference point is fixed ($\vec{a} = 0$) or is the systems center of mass ($\vec{S} = 0$). For the case of a rigid body with an attached mass, a more convenient choice of reference points is the center of mass of the main body. Mass motions can then be specified with respect to the main body center of mass instead of the system center of mass which will be moving with respect to the main body.

For the case considered here of a main body having one attached movable mass with no external torques, Equation (1) reduces to

$$\frac{d}{dt}\vec{H} + \vec{S} \times \vec{a} = 0 \tag{2}$$

The system geometry is shown in Figure 1. The angular momentum of the main body, $\vec{H}_b$, with respect to its principal axes is

$$\vec{H}_b = I_1\omega_1\hat{i} + I_2\omega_2\hat{j} + I_3\omega_3\hat{k} \tag{3}$$

where $\hat{i}$, $\hat{j}$, $\hat{k}$ are the unit vectors along the principal axes, and ω_1, ω_2 and ω_3 are the angular rates about these axes, respectively. Therefore,

$$\frac{d}{dt}\vec{H}_b = [\dot{\vec{H}}_b] + \vec{\omega}x\vec{H}_b$$

$$\begin{aligned}\frac{d}{dt}\vec{H}_b = {} & [I_1\dot{\omega}_1 + \omega_2\omega_3\ (I_3 - I_2)]\ \hat{i} \\ & + [I_2\dot{\omega}_2 + \omega_1\omega_3\ (I_1 - I_3)]\ \hat{j} \\ & + [I_3\dot{\omega}_3 + \omega_1\omega_2\ (I_2 - I_1)]\ \hat{k}\end{aligned} \tag{4}$$

This portion of Equation (2) corresponds to the normal Euler principal axes equations.

The angular momentum of the point mass with respect to the main body center of mass, $\vec{H}_m$, is

$$\vec{H}_m = \vec{H}_{\substack{\text{m about its own} \\ \text{center of mass}}} + m\vec{r} \times \frac{d\vec{r}}{dt} \tag{5}$$

With the assumption of a point mass H_m about its own center of mass is equal to zero and we may write

$$\frac{d}{dt}\vec{H}_m = m\vec{r} \times \frac{d^2\vec{r}}{dt^2}\ . \tag{6}$$

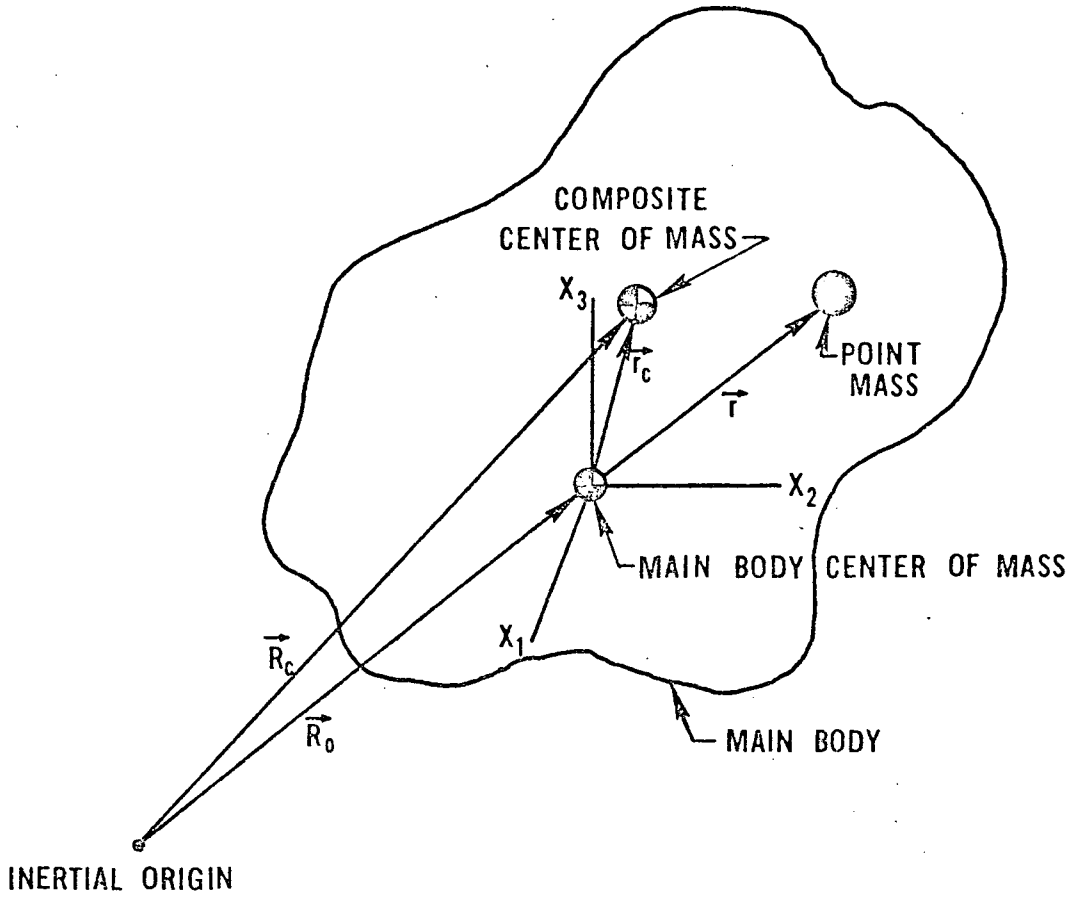

Figure 1. Main Body and Attached Mass System Geometry

The term $\frac{d^2\vec{r}}{dt^2}$ is the acceleration of the point mass with respect to the main body center of mass. From Thomson[6],

$$\frac{d^2\vec{r}}{dt^2} = \vec{\omega}x\ (\vec{\omega}\ x\ \vec{r}) + \dot{\vec{\omega}}\ x\ \vec{r} + 2\vec{\omega}\ x\ \dot{\vec{r}} + \ddot{\vec{r}}\ . \tag{7}$$

The first term of Equation (7) is the centripital acceleration, the second is the tangential acceleration, the third is the Coriolis acceleration, and the last term is the acceleration of the mass relative to the main body axes. The total angular momentum of the system with respect to the main body of mass is

$$\vec{H} = \vec{H}_b + \vec{H}_m. \tag{8}$$

The first moment of mass is given by

$$\vec{S} = m\vec{r} = m(x\hat{i} + y\hat{j} + z\hat{k}) \tag{9}$$

Note that the main body does not contribute to the term since the reference origin is its own center of mass. The inertial acceleration of the origin is from Figure (1),

$$\vec{a} \equiv \frac{d^2}{dt^2}\vec{R}_o = \frac{d^2}{dt^2}\ \vec{R}_c - \frac{d^2}{dt^2}2\vec{r}_c \tag{10}$$

Here

$$\frac{d^2}{dt^2}\vec{R}_c = \frac{\vec{F}}{M + m}$$

where F is the resultant of external forces acting on the system, M is the mass of the main body, and m is the mass of the moving mass.

From the definition of center of mass, we may write,

$$\frac{d^2}{dt^2}\vec{r}_c = \frac{m}{M+m}\frac{d^2}{dt^2}\vec{r}$$

With the assumption of no external forces, Equation (10) becomes

$$\vec{a} = -\frac{m}{M+m}\frac{d^2}{dt^2}\vec{r} \tag{11}$$

Combining Equations (6), (8), (9) and (11) into Equation (2) yields

$$\frac{d}{dt}\vec{H}_b + m\vec{r} \times \frac{d^2\vec{r}}{dt^2} + m\vec{r} \times \left(-\frac{m}{M+m}\frac{d^2\vec{r}}{dt^2}\right) = 0$$

Combining terms yields

$$\frac{d}{dt}\vec{H}_b + \frac{mM}{m+M}\vec{r} \times \frac{d^2}{dt^2}\vec{r} = 0 \tag{12}$$

It is useful to define the term

$$\mu \equiv \frac{mM}{m+M},$$

as the reduced mass, and

$$\vec{f} = \mu\frac{d^2}{dt^2}\vec{r}$$

as a "pseudo-force." Substituting these quantities into Equation (12) yields

$$\frac{d}{dt}\vec{H}_b + \mu\vec{r} \times \vec{f} = 0 \tag{13}$$

or

$$\frac{d}{dt}\vec{H}_b = -\mu\vec{r} \times \vec{f} \tag{14}$$

From Equation (14) it is apparent that the dynamics may be thought of as those of a rigid body being acted upon by a reaction "pseudo-moment" of $-\mu\vec{r} \times \vec{f}$ which is a result of mass motion.

Expanding Equation (13) yields a set of three coupled, highly non-linear differential equations for the system dynamics in terms of the angular rates of the main body (ω_1, ω_2, ω_3), the principal moments of inertia (I_1, I_2, I_3), movable mass position (x, y, z), velocity ($\dot{x}$, $\dot{y}$, $\dot{z}$), and acceleration ($\ddot{x}$, $\ddot{y}$, $\ddot{z}$). All of these quantities are with respect to the body fixed principal axes (X_1, X_2, X_3, respectively). The equations are:

$$\begin{aligned}
&\left[I_1 + \mu(y^2+z^2)\right]\dot{\omega}_1 + \left[I_3 - I_2 + \mu(y^2 - z^2)\right]\omega_2\omega_3 \\
&+ \mu\left[-xy\dot{\omega}_2 - xz\dot{\omega}_3 + (2y\dot{y} + 2z\dot{z})\omega_1 + yz(\omega_3^2 - \omega_2^2)\right. \\
&\left. - 2\dot{x}y\omega_2 - 2\dot{x}z\omega_3 - xz\omega_1\omega_2 + xy\omega_1\omega_3 + y\ddot{z} - z\ddot{y}\right] = 0
\end{aligned} \tag{15}$$

$$\begin{aligned}
&\left[I_2 + \mu(z^2+x^2)\right]\dot{\omega}_2 + \left[I_1 - I_3 + \mu(z^2 - x^2)\right]\omega_3\omega_1 \\
&+ \mu\left[-yz\dot{\omega}_3 - yx\dot{\omega}_1 + (2z\dot{z} + 2x\dot{x})\omega_2 + zx(\omega_1^2 - \omega_3^2)\right. \\
&\left. - 2\dot{y}z\omega_3 - 2\dot{y}x\omega_1 - yx\omega_2\omega_3 + yz\omega_2\omega_1 + z\ddot{x} - x\ddot{z}\right] = 0
\end{aligned} \tag{16}$$

$$[I_3 + \mu(x^2+y^2)]\dot{\omega}_3 + [I_2 - I_1 + \mu(x^2-y^2)]\omega_1\omega_2$$
$$+\mu[-2x\dot{\omega}_1 - 2y\dot{\omega}_2 + (2x\dot{x} + 2y\dot{y})\omega_3 + xy(\omega_2^2 - \omega_1^2) \qquad (17)$$
$$-2\dot{z}x\omega_1 - 2\dot{z}y\omega_2 - zy\omega_3\omega_1 + zx\omega_3\omega_2 + x\ddot{y} - y\ddot{x}] = 0$$

Thus, for prescribed motions of the control mass the resultant motion of the main body may be determined. The equations are valid irrespective of the physical mechanism whereby the control mass executes its motion.

The expanded form of the "pseudo-force", $\vec{f}$, acting on the mass and reacted to by the main body is

$$f_1 = \mu[\ddot{x} - 2\dot{y}\omega_3 + 2\dot{z}\omega_2 - y\dot{\omega}_3 + z\dot{\omega}_2 + y\omega_1\omega_2 + z\omega_1\omega_3 - x(\omega_2^2+\omega_3^2)] \qquad (18$$

$$f_2 = \mu[\ddot{y} - 2\dot{z}\omega_1 + 2\dot{x}\omega_3 - z\dot{\omega}_1 + x\dot{\omega}_3 + z\omega_2\omega_3 + x\omega_2\omega_1 - y(\omega_3^2+\omega_1^2)] \qquad (19$$

$$f_3 = \mu[\ddot{z} - 2\dot{x}\omega_2 + 2\dot{y}\omega_1 - x\dot{\omega}_2 + y\dot{\omega}_1 + x\omega_3\omega_1 + y\omega_3\omega_2 - z(\omega_1^2+\omega_2^2)] \qquad (20$$

To develop the expression for the kinetic energy of the system with respect to the composite center of the mass, consider Figure 2. The

kinetic energy is defined as follows,

$$T = \frac{1}{2} \sum_{i=1}^{N+1} m_i \frac{d\vec{r}_i}{dt} \cdot \frac{d\vec{r}_i}{dt} \tag{21}$$

where the main body is considered to consist of N masses of mass m_i and the (N + 1) mass is considered to be the control mass. From Figure 2,

$$\vec{r}_i = \vec{R}_c + \vec{\rho}_i$$

Equation (21) then becomes

$$T = \frac{1}{2} (M + m) \left(\frac{d}{dt} \vec{R}_c\right)^2 + \frac{1}{2} \sum_{i=1}^{N+1} m_i \left(\frac{d}{dt} \vec{\rho}_i\right)^2 + \frac{d}{dt} \dot{\vec{R}}_c \left(\sum_{i=1}^{N+1} m_i \frac{d}{dt} \vec{\rho}_i \right)$$

The first term us the kinetic energy of the composite center of mass, the second term is the rotational kinetic energy about the composite center of mass, and the last term is zero from the definition of the center of mass of the system. Consider only the rotational kinetic energy, therefore,

$$\begin{aligned} T_{rot} &= \frac{1}{2} \sum_{i=1}^{N+1} m_i \left(\frac{d}{dt} \vec{\rho}_i\right)^2 \\ &= \frac{1}{2} \sum_{i=1}^{N} m_i \left(\frac{d}{dt} \vec{\rho}_i\right)^2 + \frac{1}{2} m \left(\frac{d}{dt} \vec{r}_m\right)^2 \end{aligned} \tag{22}$$

From Figure 2.

$$\vec{r}_m = \vec{r} - \vec{r}_c$$

and

$$\vec{\rho}_i = \vec{\eta}_i - \vec{r}_c$$

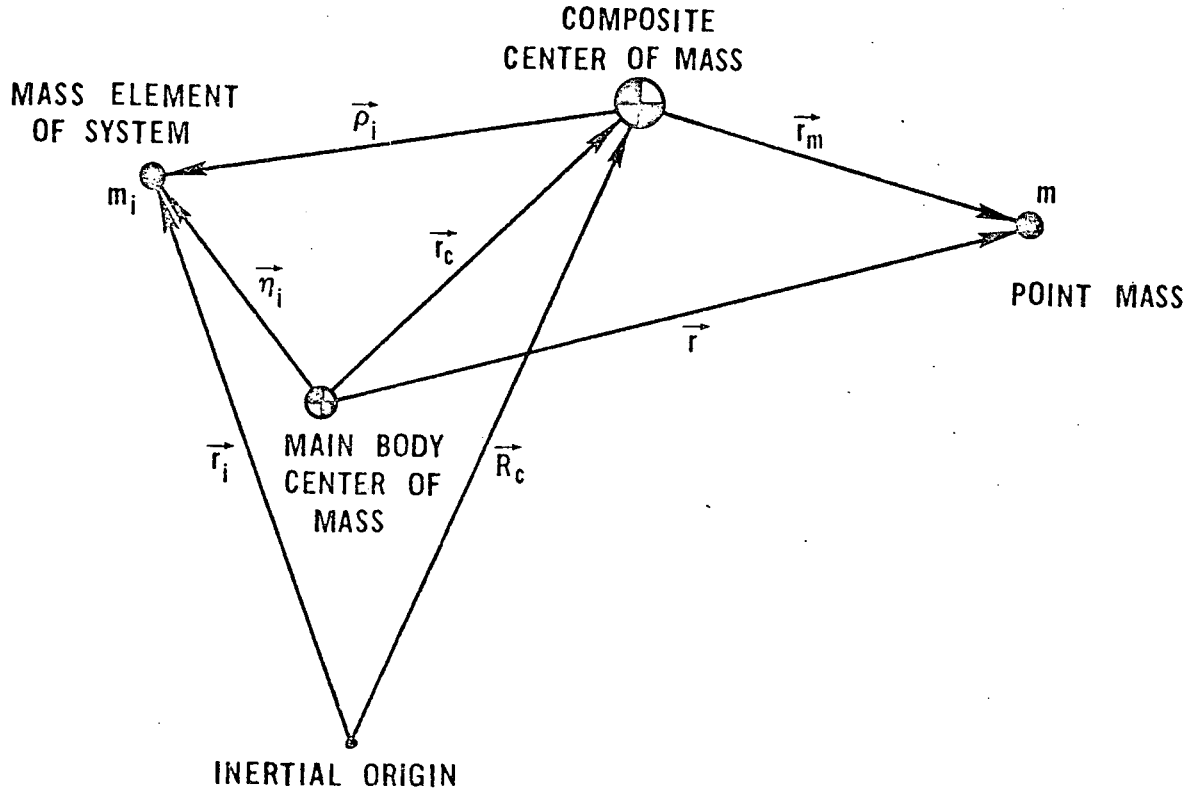

Figure 2. System Geometry for Determination of System Kinetic Energy

From the definition of center of mass,

$$\vec{r}_c = \frac{m}{M+m} \vec{r}.$$

Substituting these relations into Equation (22) and simplifying yields

$$T_{rot} = \frac{1}{2} \sum_{i=1}^{N} m_i \left(\frac{d}{dt} \vec{\eta}_i\right)^2 + \frac{1}{2} \frac{mM}{m + M} \left(\frac{d}{dt} \vec{r}\right)^2$$

The first term is the rotational kinetic energy of the main body about its own center of mass. The second term is the rotational kinetic energy of a "pseudo-mass" with respect to the main body center of mass. Therefore, the rotational kinetic energy of the system about the composite center of mass is,

$$T_{rot} = \frac{1}{2}(I_1\omega_1^2 + I_2\omega_2^2 + I_3\omega_3^2) + \frac{1}{2} \mu \left(\frac{d}{dt} \vec{r}\right)^2 \tag{23}$$

or in expanded form,

$$\begin{aligned} T_{rot} = {} & \frac{1}{2} (I_1\omega_1^2 + I_2\omega_2^2 + I_3\omega_3^2) \\ & + \frac{1}{2} \mu [(\dot{x} + z\omega_2 - y\omega_3)^2 + (\dot{y} + x\omega_3 - z\omega_1)^2 + (\dot{z} + y\omega_1 - x\omega_2)^2] \end{aligned} \tag{24}$$

The expression for angular momentum with respect to the composite center of mass may be developed similarly.[2] The result is

$$\vec{H}_c = \bar{\bar{I}} \cdot \vec{\omega} + \mu \vec{r} \times \frac{d}{dt} \vec{r}$$

where $\bar{\bar{I}}$ is the inertia dyadic. It should be remembered that $\vec{H}$ in Equation (8) is the angular momentum with respect to the main body center of mass, whereas $\vec{H}_c$ is the angular momentum with respect to the composite center of mass of the system. The equation of motion

would be

$$\frac{d}{dt}\vec{H}_c = 0 \tag{25}$$

if the composite center of mass were chosen as the origin. Since Equation (25) indicates that H_c = constant, this may be used to determine the accuracy of a numerical solution to Equations (15) - (17).

Since the movable mass control system is to decrease the kinetic energy of the spacecraft, the rate of change of the rotational kinetic energy may be developed. If Equation (24) is differentiated and simplified using Equations (15) - (17), the result is found to be independent of the main vehicle properties (I_1, I_2, I_3) and depend only on vehicle and mass motions. The result is

$$\begin{aligned}\dot{T}_{rot} = \mu\big[&-(y\dot{y}+z\dot{z})\omega_1^2 - (z\dot{z}+x\dot{x})\omega_2^2 - (x\dot{x}+y\dot{y})\omega_3^2 \\ &+ (\dot{x}y+\dot{y}x)\omega_1\omega_2 + (\dot{y}z+\dot{z}y)\omega_2\omega_3 + (\dot{x}z+\dot{z}x)\omega_1\omega_3 \\ &+ (y\ddot{z}-\dot{y}z)\omega_1 + (z\ddot{x}-\dot{z}x)\omega_2 + (x\ddot{y}-\dot{x}y)\omega_3 + (\dot{x}\ddot{x}+\dot{y}\ddot{y}+\dot{z}\ddot{z})\big]\end{aligned} \tag{26}$$

Comparing Equation (26) with Equations (18) - (20), the following relation is verified.

$$\dot{T}_{rot} = \dot{\vec{r}} \cdot \vec{f} \tag{27}$$

This surprisingly simple relationship will be used to develop a control law in the next section.

III. SELECTION OF CONTROL LAWS

Equations (15) - (17) determine the attitude motions of the spacecraft for specified motions of the control mass. It is the function

of the control law to relate the motions of the control mass to measurable vehicle parameters so that the control mass may respond to vehicle motions in an appropriate manner to lessen tumbling. A satisfactory control law should not be unnecessarily complicated. It should, however, require determination of measurable vehicle parameters, produce stable responses, and result in a final state of a simple spin about either the maximum or minimum moment of inertia axes. In the following analysis, the vehicle is assumed to have three distinct moments of inertia. I_1, I_2, and I_3 and the relationship $I_3 > I_2 > I_1$ is assigned to these quantitites.

By inspection of Equations (15) - (17), the equations of motion for an asymmetric vehicle with attached movable mass are extremely complicated due to their highly coupled and non-linear nature. Since the initial tumble rates may be large about all three axes, the equations of motion cannot be simplified by linearization. However, several simple cases were identified and will be discussed before considering the general case.

The first special case requires that the motion of the mass be along a line parallel to and offset a distance b from the X_3 axis and passing through the X_2 axis. Equation (15) becomes

$$[I_1 + \mu(b^2 + z^2)]\,\dot{\omega}_1 + [I_3 - I_2 + \mu(b^2 - z^2)]\,\omega_2\omega_3 + 2\mu z\dot{z}\omega_1 + \mu b z(\omega_3^2 - \omega_2^2) + \mu b\ddot{z} = 0 \tag{28}$$

Suppose the control law is chosen such that

$$z = c\omega_1. \tag{29}$$

Substituting this into Equation (28) with the assumption, $I_1 >> \mu c^2 \omega_1^2$, Equation (28) becomes

$$\ddot{\omega}_1 + \frac{[I_1 + \mu b^2]}{\mu bc} \dot{\omega}_1 + (\omega_3^2 - \omega_2^2)\, \omega_1 = \frac{[I_2 - I_3 - \mu b^2]}{\mu bc} \omega_2 \omega_3 \qquad (30)$$

Equation (30) indicates for the case where $\omega_3 > \omega_2$, Equation (29) will result in damping of ω_1 to zero producing a stable spin about the maximum moment of inertia axis. The control law given by Equation (29) would be easy to implement, requiring measurement of only z and ω_1. The mass would oscillate about its equilibrium position with decreasing amplitudes since ω_1 would be damped. The control mass would return to its zero position when ω_1 equals zero and a flat spin is reached. For the case of an arbitrary tumbling spacecraft, the assumption $\omega_3 > \omega_2$ cannot be made and Equation (29) does not provide a satisfactory control law. However, the result may be useful in designing a control system for a space station which has an artificial -g mode where the spacecraft has a large rate about one axis, say ω_3, and the control system is to damp out small transverse rates.

Since a flat spin about the maximum moment of inertia axis is the minimum energy state of the system, it is evident that Equation (29) produces a dissipation of energy. The second specialized case demonstrates that a movable mass control system may increase the energy of the system to the maximum energy state. The vehicle would,

therefore, be in a flat spin about its minimum moment of inertia axis. For this case the motion is to be along a line oriented parallel to and offset by some distance (a) from the X_1 axis and passing through the X_2 axis. For this configuration Equation (17) becomes

$$[I_3 + \mu(x^2 + b^2)]\,\dot{\omega}_3 + [I_2 - I_1 + \mu(x^2 - b^2)]\,\omega_1\omega_2 + 2\mu x\dot{x}\omega_3 + \mu b x(\omega_2^2 - \omega_1^2) - \mu b\ddot{x} = 0 \tag{31}$$

Suppose the control law is now chosen to be

$$x = c\omega_3. \tag{32}$$

With this choice of control law and the assumption $I_2 >> \mu c^2\omega_3^2$, Equation (31) becomes

$$\ddot{\omega}_3 - \frac{[I_3 + \mu b^2]}{\mu bc}\,\dot{\omega}_3 + (\omega_1^2 - \omega_2^2)\,\omega_3 = \frac{[I_2 - I_1 + \mu b^2]}{\mu bc}\,\omega_1\omega_3 \tag{33}$$

Equation (33) indicates that if the product (bc) is chosen such that ($bc < 0$) and the special case of $\omega_1 > \omega_2$, Equation (32) will result in damping of ω_3 to zero and produce a flat spin about the minimum moment of inertia axis (X_1). The properties of the control law are similar to those of Equation (29).

The two preceding examples have demonstrated that the movable mass control system may increase or decrease the energy of the system and produce a flat spin about either the minimum or maximum moment of inertia axis. They also indicate that possibly the proper orientation for the direction of motion of the control mass is parallel to

the desired final spin axis. However, since the initial tumble state of the vehicle is not known, the necessary assumptions may not be made for the general case of tumbling. The control laws given by Equations (29) and (32) are, therefore, attractive but inadequate in their simplicity. Therefore, a control law was searched for which would result in a flat spin, irregardless of initial conditions. It was also determined that although the control system could possibly force a flat spin about the minimum moment of inertia axis, the control system should produce a flat spin about the maximum moment of inertia axis due to its inherent stability in the presence of dissipative forces.

The development of the control law starts with the theory of Liapunov stability. From Reference 7, the system of differential equations produced by Equations (15) - (17) and the control law which is selected is completely stable and approaches its minimum state if there exists a scalar function, $V(x)$, where x is the state vector of the system, if

1) $V(x) > 0$ for all $x \neq 0$

2) $\dot{V}(x) \leq 0$ for all x

3) $V(x) \to \infty$ as $|| x || \to \infty$.

For physical systems, a convenient scalar function to use as a Liapunov function ($V(x)$), is the rotational kinetic energy of the system due to its inherent positive definiteness which satisfies conditions (1) and (3). The rate of change of rotational kineticenergy

is given by Equation (27) which is repeated here.

$$\dot{T}_{rot} = \dot{\vec{r}} \cdot \vec{f} \tag{34}$$

Consider the case where the control mass is restricted to move along a line parallel to the X_3 axis, and offset from this axis as shown in Figure 3. For this case Equation (34) simplifies to

$$\dot{T}_{rot} = \dot{z} f_3. \tag{35}$$

Thus, if the control law is chosen such that

$$f_3 = - \mu c \dot{z} \tag{36}$$

Equation (35) becomes

$$T_{rot} = - \mu c \dot{z}^2 \tag{37}$$

which satisfies condition (2). Using Equations (36) and (20), the resulting equation of motion for the mass is

$$\ddot{z} + c\dot{z} - (\omega_1^2 + \omega_2^2)\, z = a\dot{\omega}_2 - b\dot{\omega}_1 - a\omega_3\omega_1 - b\omega_2\omega_3 \tag{38}$$

This equation would decrease the kinetic energy of the system, and the forcing function of Equation (38) would vanish when a final spin about the X_3 axis would be reached. However, due to the negative, decaying coefficient of the "z" term, the mass would not necessarily return to its equilibrium position (z = 0). Therefore, it is desirable to modify Equation (36) to return the control mass to its zero position. If the control law is chosen such that

$$f_3 = - \mu c_1 \dot{z} - \mu z (c_2 + \omega_1^2 + \omega_2^2), \tag{39}$$

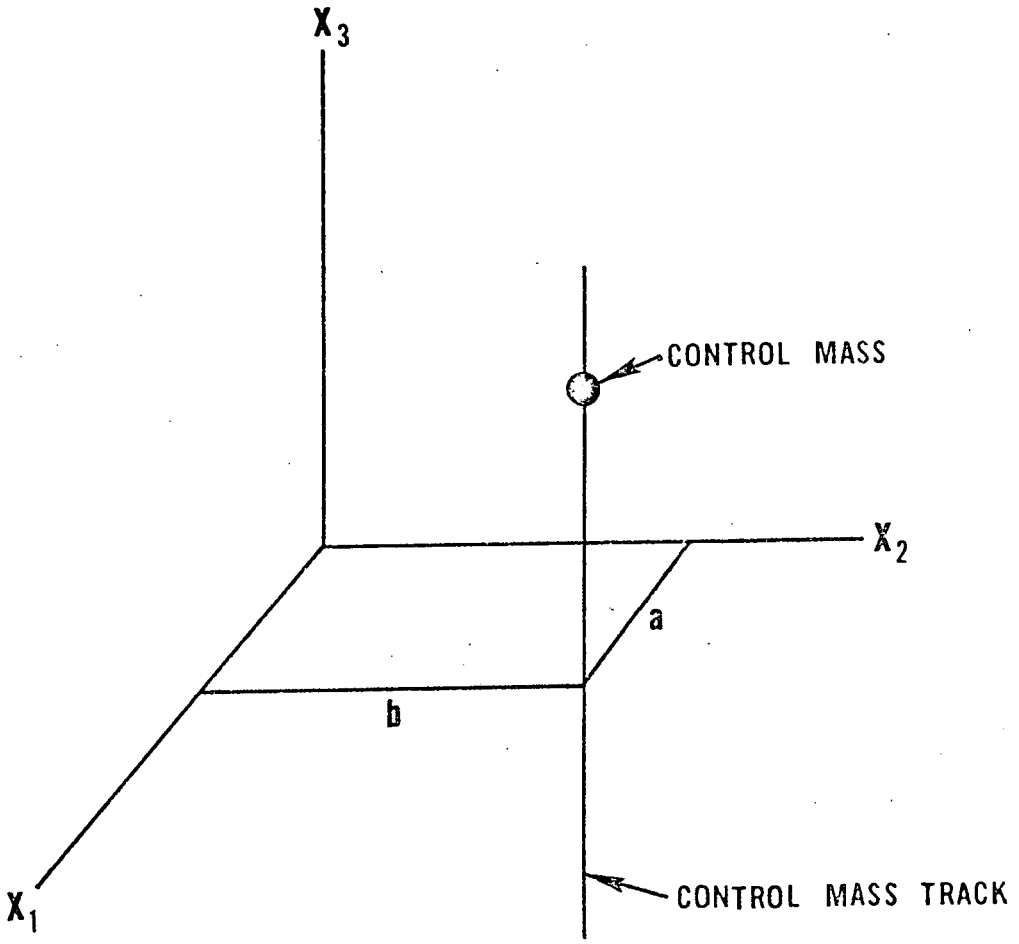

Figure 3. Orientation of Control Mass Path

the equation for the mass motion becomes

$$\ddot{z} + c_1\dot{z} + c_2 z = a\dot{\omega}_2 - b\dot{\omega}_1 - a\omega_3\omega_1 - b\omega_2\omega_3 \tag{40}$$

For this selection of control law

$$\dot{T}_{rot} = - \mu c_1 \dot{z}^2 - \mu z\dot{z}(c_2 + \omega_1^2 + \omega_2^2). \tag{41}$$

Here, the formulation departs from the Liapunov method since the second term of Equation (41) is not negative semi-definite. Since the first term will be decreasing the energy and the second term will be oscillatory, increasing and decreasing the energy, and if the c_1 and c_2 are chosen properly the secular negative semi-definite term will dominate. In the next section it will be shown that while during a small part of the mass cycle $\dot{T} > 0$, the $\dot{T} < 0$ portion dominates over the complete cycle. If every mass cycle has a net negative value for $\dot{T}$, the system will approach its minimum energy state and be in a flat spin about the maximum moment of inertia axis. From Equation (40), the mass will be back at its zero position.

IV. RESULTS

To demonstrate the feasibility of the movable mass control system using the control law given by Equation (39), the Modular Space Station (MSS) was chosen as an example vehicle. The properties of the MSS are listed below.

I_1 = 5,152,800 kgm^2 (3,799,958 slug ft^2)

I_2 = 6,275,568 kgm^2 (4,627,993 slug ft^2)

I_3 = 6,742,032 kgm^2 (4,972,048 slug ft^2)

M = 99,792 kg (220,000 lb)

The weight of the control mass was arbitrarily chosen to be 0.1% of the MSS mass.

m = 99.792 kg (220 lb)

The offset distances, (a) and (b), and the constants, (c_1) and (c_2) were arbitrarily chosen to be

a = 9.144 m (30 ft)

b = 9.144 m (30 ft)

c_1 = 1.0 sec^{-1}

c_2 = 0.01 sec^{-2}

The initial rotation rates were arbitrarily chosen to be

$\omega_1(0) = \omega_2(0)$ = 0.955 rpm

$\omega_3(0)$ = 4.0 rpm

Using equations (15), (16), (17), and (40) with the above choice of parameter values, the system of differential equations was solved using a fourth order Runge-Kutta algorithm on the IBM 360 computer. The results are shown in Figures 4 and 5.

Figure 4 shows the envelopes formed by the oscillations of the ω's. As can be seen from Figure 4, ω_1 and ω_2 oscillate with decreasing amplitudes while ω_3 approaches its steady state spin value. The envelope of oscillation of the control mass is shown in Figure 5. As can be

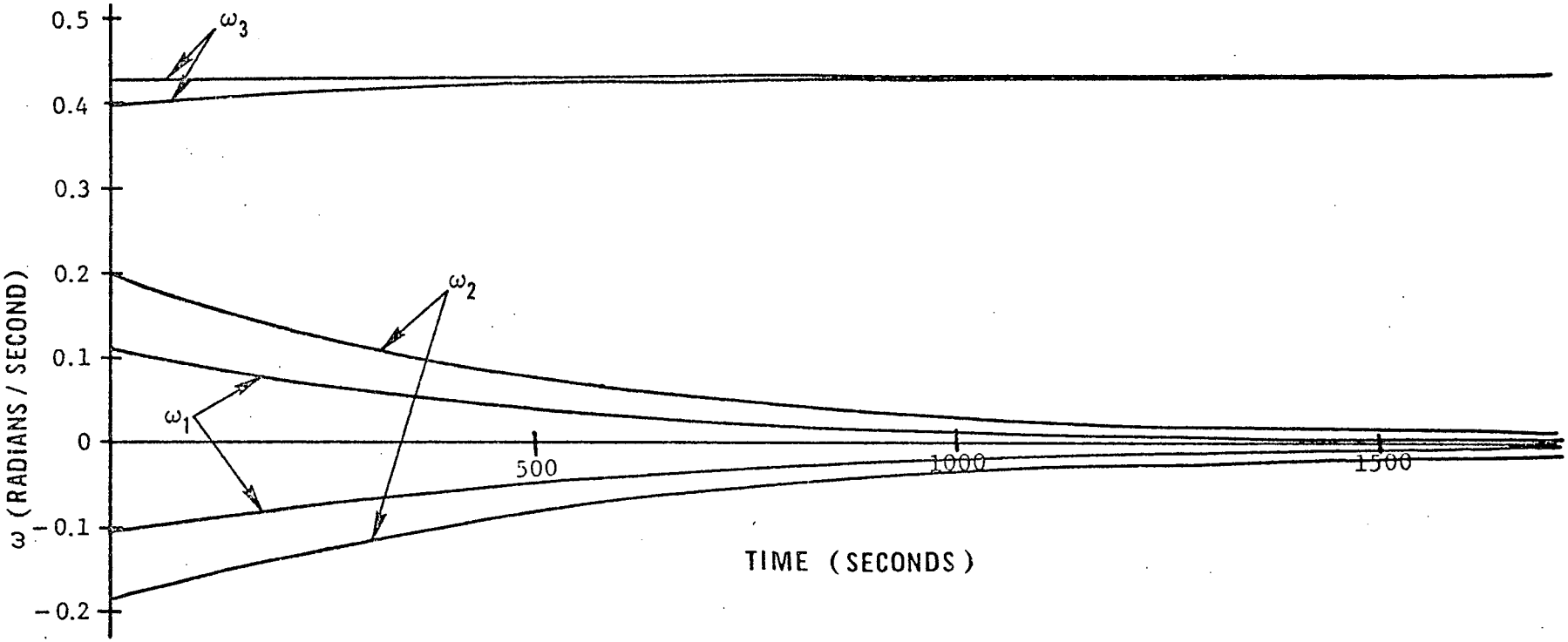

Figure 4. Envelopes of ω Oscillations

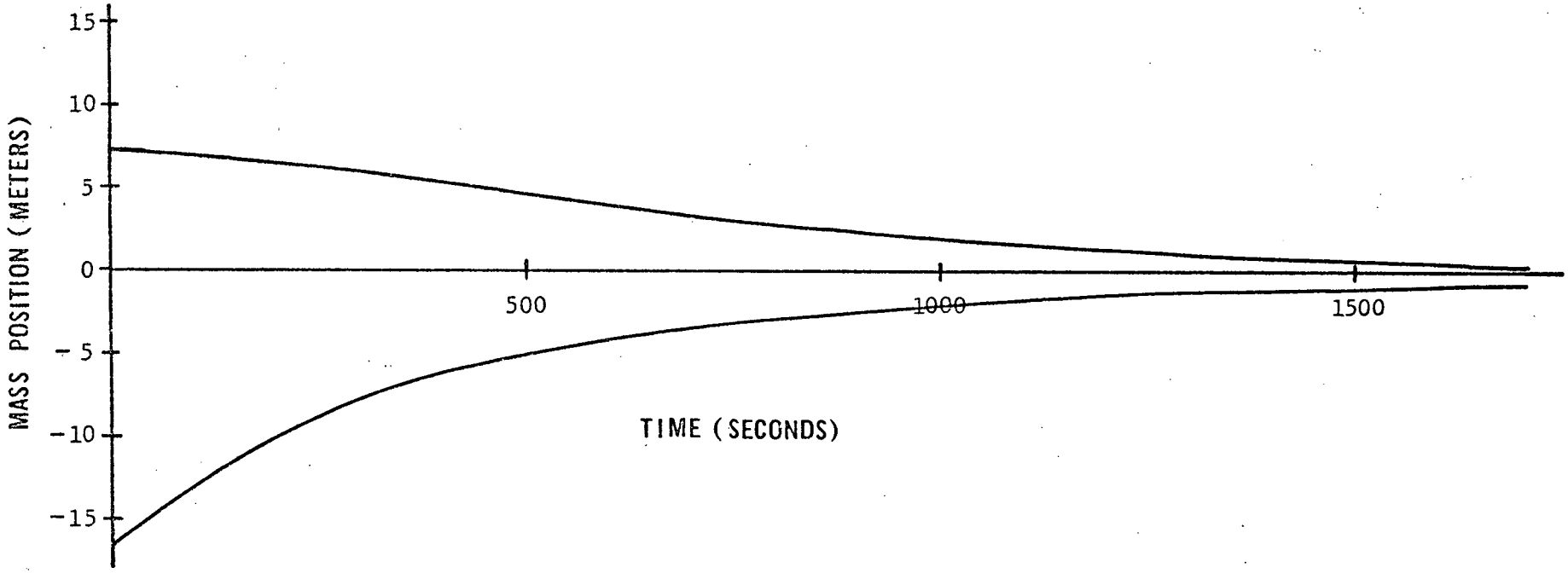

Figure 5. Mass Oscillation Envelope

seen from this figure, the control mass oscillates about its zero position with decreasing amplitude which approaches zero. Thus, the ability of the movable mass control system, using the control law given by Equation (39), to reduce arbitrary tumbling to a simple spin about the maximum moment of inertia axis has been demonstrated. From the computer results, it was found that over a small portion of the mass oscillation cycle the rate of change of rotational kinetic energy was positive. Over the entire cycle, the negative contribution dominates and results in a net decrease in kinetic energy. While the maximum amplitude of the mass oscillation may be excessive for this case (15m), the maximum amplitude may be adjusted by a proper choice of the parameters c_1 and c_2.

The rate of change of kinetic energy is given by Equation (41) which is repeated here

$$\dot{T} = - \mu c_1 z^2 - \mu z z (c_2 + \omega_1^2 + \omega_2^2) \tag{41}$$

From Equation (41) it seems that for a large rate of change of kinetic energy and, hence, fast approach to a simple spin, the parameter c_1 should be chosen large and c_2 should be chosen small. However, consider the left hand side of Equation (40).

$$z + c_1 z + c_2 z = F(\dot{\omega}, \omega) \tag{42}$$

Equation (42) may be thought of as the equation for the forced motion of a spring-mass-damper system. In this analogy, c_1 corresponds to the damping constant of the damper and c_2 corresponds to the spring

constant. If c_1 is chosen large as Equation (41) indicates, this increases the damper strength and limits the velocity of the control mass. Since the first term of Equation (41) is $\mu c_1 z^2$, an increase in c_1 may result in a net decrease in the magnitude of this term. Also, if c_2 is chosen small as Equation (41) indicates, this decreases the spring strength and increases the amplitude of oscillation of the control mass. Thus, it can be seen that the parameters c_1 and c_2 must be chosen carefully, considering not only their effect on Equation (41) but also their effect on Equation (42). Effort is being directed towards finding an analytical method for choosing these parameters.

V. CONCLUSIONS

A movable mass control system to convert the tumbling motions of a spacecraft into a simple spin has been studied. The equations of motion of a rigid spacecraft with attached control mass have been formulated and a control law has been selected. For an example, spacecraft and initial conditions it has been shown that the movable mass control system is capable of decreasing the kinetic energy of the system to its minimum value and result in a simple spin about the maximum moment of inertia axis within one hour. This control system would become active upon loss of control. Future work will be directed toward establishing control system sensors, power, and energy requirements. Also, work will be directed towards establishing analytical methods for choosing control system parameters to obtain a control system which operates within established limits of mass amplitude and other constraints while still detumbling the spacecraft in a reasonable

time. Also, methods of despinning the spacecraft after a simple spin state is reached will be investigated as to their feasibility and practicality.

VI. REFERENCES FOR APPENDIX B

1. Grubin, C., "Dynamics of a Vehicle Containing Moving Parts," Trans. of the ASME, Journal of Applied Mechanics, Vol. 29, No. 3, September 1962, pp. 486-488.

2. Roberson, R. E., "Torques on a Satellite Vehicle from Internal Moving Parts," Trans. of the ASME, Journal of Applied Mechanics, Vol. 25, June 1958, pp. 196-200.

3. Kane, T. R. and Scher, M. P., "A Method of Active Attitude Control Based on Energy Considerations," J. of Spacecraft, Vol. 6, No. 5, May 1969, pp. 633-636.

4. Childs, D. W., "A Movable-Mass Attitude - Stabilization System for Artificial-g Space Stations," J. of Spacecraft, Vol. 8, No. 8, August 1971, pp. 829-834.

5. Lorell, K. R., and Lange, B. O., "An Automatic Mass-Trim System for Spinning Spacecraft," AIAA Journal, Vol. 10, No. 8, August 1972, pp. 1012-1015.

6. Thomson, W. T., Introduction to Space Dynamics, John Wiley and Sons, Inc., New York, 1963, pp. 22.

7. LaSalle, J. P., "Some Extensions of Liapunov's Second Method," IRE Transactions on Circuit Theory, December 1960, pp. 520-527.

APPENDIX C

OPTIMIZATION OF MOVABLE MASS CONTROLS

I. INTRODUCTION

A general time history of internal control mass motion in a tumbling space vehicle to achieve simple spin about an axis of the body is not available. It would seem feasible to use optimization techniques to solve the nonlinear differential equations with initial and final conditions on the state variables. Time minimization was initially attempted. However, the minimum time condition was being satisfied at the cost of the mass position constraining penalty function. The optimization was subsequently changed to minimization of the mass position for a fixed time. This change yields better results, but further work yet remains in order to obtain satisfactory mass position time histories that convert tumbling to simple spin.

II. ANALYSIS

The vector equation of motion for a rigid body with internal mass movement whose coordinate system is located at the center of mass is [1]

$$\vec{M} = \dot{\vec{H}} + \vec{S} \times \vec{a}$$

where

$\vec{M}$ = External moment

$\vec{H}$ = Angular momentum of the spacecraft including the movable mass

$\vec{S}$ = First moment of mass of the system

$\vec{a}$ = Acceleration of the spacecraft center of mass (not including the movable mass).

Therefore, for no external torque, the equations governing the motion of a spacecraft with a movable mass (along the x axis) for a body fixed, spacecraft (less mass) center of mass located coordinate system are

$$\dot{\omega}_x = \left[VAA\left(X^2\,CMA1 + X^4\,CMA2 + CMA3\right) + VBB\left(X\,CMB1 + X^2\,CMB2 + X^3\,CMB3 + CMB4\right) + VCC\left(X\,CMC1 + X^2\,CMC2 + X^3\,CMC3 + CMC4\right)\right]\left[1.0/|\underline{A}|\right]$$

$$\dot{\omega}_y = \left[VAA\left(X\,CNA1 + X^2\,CNA2 + X^3\,CNA3 + CNA4\right) + VBB\left(X\,CNB1 + X^2\,CNB2 + CNB3\right) + VCC\left(X\,CNC1 + X^2\,CNC2 + CNC3\right)\right]\left[1.0/|\underline{A}|\right]$$

$$\dot{\omega}_z = \left[VAA\left(X\,CPA1 + X^2\,CPA2 + X^3\,CPA3 + CPA4\right) + VBB\left(X\,CPB1 + X^2\,CPB2 + CPB3\right) + VCC\left(X\,CPC1 + X^2\,CPC2 + CPC3\right)\right]\left[1.0/|\underline{A}|\right]$$

where

$$VAA = \omega_y^2\,CWA1 + \omega_z^2\,CWA2 + \omega_x\omega_y\left(CWA3 + X\,CWA4\right) + \omega_x\omega_z\left(CWA5 + X\,CWA6\right) + \omega_y\omega_z\,CWA7 + \omega_y\dot{X}\,CWA8 + \omega_z\dot{X}\,CWA9$$

$$VBB = \omega_x^2\left(CWB1 + X\,CWB2\right) + \omega_z^2\left(CWB3 + X\,CWB4\right) + \omega_x\omega_y\,CWB5 + \omega_x\omega_z\left(CWB6 + X^2\,CWB7\right) + \omega_y\omega_z\left(CWB8 + X\,CWB9\right) + \omega_y X\dot{X}\,CWB10 + \ddot{X}\,CWB11$$

$$VCC = \omega_x^2 \left(CWC1 + X\, CWC2 \right) + \omega_y^2 \left(CWC3 + X\, CWC4 \right)$$
$$+ \omega_x \omega_y \left(CWC5 + X^2\, CWC6 \right) + \omega_x \omega_z\, CWC7$$
$$+ \omega_y \omega_z \left(CWC8 + X\, CWC9 \right) + \omega_z X \dot{X}\, CWC10$$
$$+ \ddot{X}\, CWC11$$

$$|\underline{A}| = X^4 \mu^2\, CA3 + X^3\, CA23 + X^2 \mu\, CA2 + X\, CA12 + CA1$$

$$CA3 = I_x$$

$$CA23 = -2 I_{xy} \mu^2 y - 2 I_{xz} \mu^2 z$$

$$CA2 = I_x I_y + I_x I_z - I_{xy}^2 - I_{xz}^2 + I_x \mu y^2$$
$$+ I_x \mu z^2 + I_y \mu y^2 + I_z \mu z^2 - 2 I_{yz} \mu y z$$

$$CA12 = -2 I_{xy} I_{yz} \mu z - 2 I_{xy} \mu^2 y z^2 - 2 I_{xy} I_z \mu y$$
$$- 2 I_{xy} \mu^2 y^3 - 2 I_{yz} I_{xz} \mu y - 2 I_{xz} \mu^2 y^2 z$$
$$- 2 I_{xz} I_y \mu z - 2 I_{xz} \mu^2 z^3$$

$$CA1 = I_x I_y I_z - I_x I_{yz}^2 - I_{xy}^2 I_z - I_{xz}^2 I_y$$
$$- 2 I_{xy} I_{xz} I_{yz} + I_x I_y \mu y^2 + I_x I_z \mu z^2$$
$$- 2 I_x I_{yz} \mu y z + I_y I_z \mu y^2 + I_y I_z \mu z^2$$
$$+ I_y \mu^2 y^4 + I_y \mu^2 y^2 z^2 + I_z \mu^2 y^2 z^2 + I_z \mu^2 z^4$$
$$- I_{yz}^2 \mu y^2 - I_{yz}^2 \mu z^2 - 2 I_{yz} \mu^2 y^3 z$$
$$- 2 I_{yz} \mu^2 y z^3 - I_{xy} I_{xz} \mu y z - I_{xy}^2 \mu y^2$$
$$- I_{xz} I_{xy} \mu y z - I_{xz}^2 \mu z^2$$

$CWA1 = I_{yz} + \mu y z$

$CWA2 = -I_{yz} - \mu y z$

$CWA3 = I_{xz}$

$CWA4 = \mu z$

$CWA5 = -I_{xy}$

$CWA6 = -\mu y$

$CWA7 = I_y - I_z - \mu y^2 + \mu z^2$

$CWA8 = 2\mu y$

$CWA9 = 2\mu z$

$CWB1 = -I_{xz}$

$CWB2 = -\mu z$

$CWB3 = I_{xz}$

$CWB4 = \mu z$

$CWB5 = -I_{yz} - \mu y z$

$CWB6 = I_z - I_x - \mu z^2$

$CWB7 = \mu$

$CWB8 = I_{xy}$

$CWB9 = \mu y$

$CWB10 = -2\mu$

$CWB11 = -\mu z$

$CWC1 = I_{xy}$

$CWC2 = \mu y$

$$CWC3 = -I_{xy}$$
$$CWC4 = -\mu y$$
$$CWC5 = -I_y + I_x + \mu y^2$$
$$CWC6 = -\mu$$
$$CWC7 = I_{yz} + \mu yz$$
$$CWC8 = -I_{xz}$$
$$CWC9 = -\mu z$$
$$CWC10 = -2\mu$$
$$CWC11 = \mu y$$
$$CMA1 = I_y \mu + I_z \mu + \mu^2 y^2 + \mu^2 z^2$$
$$CMA2 = \mu^2$$
$$CMA3 = I_y I_z + I_y \mu y^2 + I_z \mu z^2 - I_{yz}^2 - 2 I_{yz} \mu yz$$
$$CMB1 = I_{yz} \mu z + \mu^2 z^2 y + I_z \mu y + \mu^2 y^3$$
$$CMB2 = I_{xy} \mu$$
$$CMB3 = \mu^2 y$$
$$CMB4 = I_{yz} I_{xz} + I_{xz} \mu yz + I_{xy} I_z + I_{xy} \mu y^2$$
$$CMC1 = I_{yz} \mu y + \mu^2 y^2 z + I_y \mu z + \mu^2 z^3$$
$$CMC2 = I_{xz} \mu$$
$$CMC3 = \mu^2 z$$
$$CMC4 = I_{xy} I_{yz} + I_{xy} \mu yz + I_y I_{xz} + I_{xz} \mu z^2$$
$$CNA1 = I_{yz} \mu z + \mu^2 y z^2 + I_z \mu y + \mu^2 y^3$$
$$CNA2 = I_{xy} \mu$$
$$CNA3 = \mu^2 y$$
$$CNA4 = I_{yz} I_{xz} + I_{xz} \mu yz + I_{xy} I_z + I_{xy} \mu y^2$$
$$CNB1 = -2 I_{xz} \mu z$$

$$CNB2 = I_x \mu + \mu^2 y^2$$

$$CNB3 = I_x I_z + I_x \mu y^2 + I_z \mu y^2 + \mu^2 y^4 + I_z \mu z^2 + \mu^2 y^2 z^2 - I_{xz}^2$$

$$CNC1 = I_{xz} \mu y + I_{xy} \mu z$$

$$CNC2 = \mu^2 y z$$

$$CNC3 = I_{xz} I_{xy} + I_x I_{yz} + I_x \mu y z + I_{yz} \mu y^2 + \mu^2 y^3 z + I_{yz} \mu z^2 + \mu^2 y z^3$$

$$CPA1 = I_{yz} \mu y + \mu^2 y^2 z + I_y \mu z + \mu^2 z^3$$

$$CPA2 = I_{xz} \mu$$

$$CPA3 = \mu^2 z$$

$$CPA4 = I_{xy} I_{yz} + I_{xy} \mu y z + I_y I_{xz} + I_{xz} \mu z^2$$

$$CPB1 = I_{xz} \mu y + I_{xy} \mu z$$

$$CPB2 = \mu^2 y z$$

$$CPB3 = I_{xz} I_{xy} + I_x I_{yz} + I_x \mu y z + I_{yz} \mu y^2 + \mu^2 y^3 z + I_{yz} \mu z^2 + \mu^2 y z^3$$

$$CPC1 = -2 I_{xy} \mu y$$

$$CPC2 = I_x \mu + \mu^2 z^2$$

$$CPC3 = I_x I_y + I_x \mu z^2 + I_y \mu y^2 + \mu^2 y^2 z^2 + I_y \mu z^2 + \mu^2 z^4 - I_{xy}^2$$

$$\mu = \frac{m M}{m + M}.$$

The basic symbols used above are

ω_x = angular velocity about the x axis

ω_y = angular velocity about the y axis

ω_z = angular velocity about the z axis

x = position of the movable mass from the center of mass of the spacecraft (less this mass)

$\dot{x}$ = dx/dt

$\ddot{x}$ = d^2x/dt^2

m = mass of movable body

M = mass of spacecraft less that of the movable mass

y = position on y axis of the movable mass

z = position on z axis of the movable mass

I_x, I_y, I_z = moments of inertia

I_{xy}, I_{xz}, I_{yz} = products of inertia.

The equations of motion were put in a form necessary for the application of optimization technqiues by substituting β for $\dot{x}$ and u for $\dot{\beta}$ and adding two more first order differential equations

$$\dot{x} = \beta$$

$$\dot{\beta} = u.$$

The term u is now the control variable and ω_x, ω_y, ω_z, x and β are the state variables.

The solution of the five first order differential equations for $\omega_y(t_b)$ and $\omega_z(t_b)$ approaching zero (terminal conditions) was obtained by minimizing the x position with a first order gradient method.[2] A first order gradient method must be used since the initial guess of control histories may be far from the optimal. The parameter to be optimized was written as

$$J = \int_{t_o}^{t_b} \frac{1}{2} \frac{x^2}{x^2_{max}} \, dt.$$

III. RESULTS

The approach listed above was attempted for various postions and movement axis of the mass. The best results for the space station, as far as least maximum mass position is concerned, were for the mass moving along

the z axis of the NAR coordinate system and displaced +15 feet on NAR y axis and -15 feet in the NAR x axis. This position of the mass necessitates an external tube for the mass, but it provides for greater maximum positions and greater displacement on all axes from the space station center of mass. For initial angular velocities of ω_x = .176 rad/sec, ω_y = .097 rad/sec and ω_z = .096 rad/sec (based on axis used in equation derivation), the maximum position of a mass 1% the weight of the space station required to reduce the angular velocity on the y and z axes by 10% is over 400 ft. from the spacecraft center of mass; but, the terminal time set was 35 sec. Indications of other digital computer runs indicates that increasing the terminal time permits lower maximum mass positions. The example mentioned above required 200 sec of computer time. However, setting a terminal time of 5 to 10 minutes, as seems necessary to keep the mass position small, necessitates very large computer time.

IV. CONCLUSIONS

Minimizing mass position gave the best results to date. However, the computer time that seems necessary to arrive at satisfactory results will be very large. Attempts will be made to lower the computer time needed to solve the equations of motion for fixed terminal time. Also, the optimization techniques will be refined. The feasibility of using a hybrid computer will be investigated. One of these approaches may yield the tools needed to reduce tumbling to simple spin by using a low weight movable mass moving inside the spacecraft.

V. REFERENCES FOR APPENDIX C

1. Grubin, C., "Dynamics of a Vehicle Containing Moving Parts," Trans. of the ASME, Journal of Applied Mechanics, Vol. 29, No. 3, September 1962, pp. 486-488.

2. Bryson, Arthur E., Jr., and Ho, Yu-Chi, Applied Optimal Control, Ginn and Company, Massachusetts, 1969.

APPENDIX D

FLEXIBILITY ANALYSES AND SIMULATIONS

I. INTRODUCTION

Consider the possibility that a future manned space vehicle assumed an uncontrollable, tumbling mode of motion. In order to detumble the spacecraft to a state of simple spin about one axis, a certain amount of energy must be extracted from the tumbling craft. This appendix deals with an inherent source of energy dissipation; the energy associated with the elastic deformation of flexible appendages. Though the rate of energy dissipation due to flexibility effects is small, its magnitude will be examined. The effects of increasing the amount of flexibility, the number of elastic appendages and the size of the flexible appendages on a tumbling spacecraft is the primary consideration here. Future spacecraft design should take into account the effect flexibility has on control systems and overall spacecraft dynamics.

Many methods have been employed to study the motion of nonrigid spacecraft. An extensive review of the techniques used in dealing with flexibility has been previously completed.[1] Reviewing the "state of the art" of mathematical formulation of nonrigid spacecraft each formulation would fall into one of three categories: (1) discrete coordinate formulation; (2) vehicle normal-mode coordinate formulation; and (3) hybrid-coordinate formulation. Each of these categories can describe the mathematical analysis to be used when a spacecraft is

modelled as one of the following: (1) a collection of rigid bodies; (2) a quasi-rigid body; or (3) an elastic body.

Many spacecraft are simple in nature and they can be modelled as a collection of rigid bodies. The motion of the spacecraft would be described by a discrete-coordinate formulation. Since relative motion between the rigid bodies takes place under general motion energy dissipation from the system can be expected and is described either by the use of the energy sink method or a damping factor associated with a damping device. (e.g. a spring-mass damping mechanism). The energy sink method assumes that a definite quantity of energy will be dissipated from the system over a set interval of time in the absence of external forces or torques on the system. This can be done with good results whenever the rate of energy dissipation is small. In the cases where elastic deformation of flexible appendages are small, the energy sink method has been employed to describe the energy dissipation due to the elastic deformations. The subsequent analysis of the spacecraft attittude motion can then be accomplished.[2]

The discrete-parameter formulation of the spacecraft is still the most accurate method. However, when the space vehicles become large and more rigid bodies are needed to model it, this approach becomes impractical from the computational point of view.

If the space vehicle were completely elastic (e.g. a slender missile), a normal mode formation could be used. The vehicle normal mode formulation was described in reference (1) and is not used in this report.

A space vehicle with flexible appendages can be modelled as a quasi-rigid body. The mathematical formulation used to describe the spacecrafts motion is a hybrid-ccordinate method. This method is used in this report to analyze the effects of flexibility. The hybrid-coordinate formulation combines the generality of the discrete-coordinate approach and the computational advantages of modal coordinates. By using the hybrid coordinate formulation, it is possible to describe the rigid main body by discrete coordinates and the flexible motion of the appendages by normal mode coordinates.[3]

Quasi-coodinates are quantities whose differentials may be written as linear combinations of differentials of generalized coordinates and time.[4] Lagrange's equations of motion in terms of quasi-coordinates are used to describe the motion of the whole vehicle. The appendage's equations of motion are obtained from Lagrange's formulation using generalized coordinates associated with the normal mode method. This approach is still quite general in modelling flexible appendages. Should the vehicle have internal damping mechanisms or external torques, this approach will accommodate these possibilities. However, the present problem excludes all other types of energy dissipation mechanisms except flexibility effects and assumes no external torques are present. The tumbling space-station will therefore be experiencing moment-free motion. The generality of problem is increased by assuming an asymmetric main body. The motion of a rigid asymmetric body under a moment-free condition is mathematically described by eilliptical functions and

geometrically by a Poinsot ellipsoid rolling without slipping on an invariable plane.[2]

The hybrid-coordinate formulation has the means of incorporating damping.

Knowledge about how materials dissipates energy and provide damping in dynamical systems is still incomplete. The mathematical description of damping is only approximate at best. In the next Section, a discussion of damping factors in elastic systems will be presented. It will show how to incorporate a structural damping factor into the hybrid coordinate formulation. The structural damping factor can be and will be used in the Lagrangian formulation of the flexible appendages. Structural damping will model the means by which energy will be dissipated from the system. Due to this damping term, the deflections of the appendages will decrease. This will cause changes in the angular velocities about the three body axes of the tumbling space vehicle. It is these changes which are being investigated in this study.

Three configurations of a space station with flexible appendages will be analyzed in this work. The first will be an asymmetric rigid main body with four symmetrically placed beams about the axis of greatest moment of inertia. (See Figure 1). The second will be an asymmetric rigid body with three beams placed symmetrically about the axis of greatest moment of inertia. Here, two beams are placed along the axis of greatest moment of inertia. The third configuration will be the NAR modular space station with the large solar arrays.

The work that has been completed concerning these three configurations will be presented in this report. Theory and background material relevant to this study will also be given.

II. ENERGY DISSIPATION MODELLING

All realistic structures constitute a nonconservative system to maintain a constant energy, an external source must supply energy to the system at a rate equal to the rate of energy dissipation.

While mass and stiffness are inherent characteristics of a system, damping or the forces which dissipates energy may not be classified as such from the outset. Damping forces may depend upon the vibrating system as well as on elements exterior to it. The formulation of expressions for the damping forces poses a difficult problem that still requires extensive research. The nature of damping is usually described as one of the following: a) structural damping; b) viscous damping; c) coulomb damping.

Structural damping is due to the internal friction within the material or at connections between elements of a structural system. The resulting damping dorces are usually given as functions of strain, amplitude of deflection, or frequency of vibration.

Viscous damping is the force which impedes vibrational motion in a fluid. Viscous damping is expressed as; $F_D = c_j \dot{u}_j$ in which the constant c_j characterizes the jth damping mechanism.

Coulomb or dry-friction damping results from the motion of a body on a dry surface. In a space vehicle structure, Coulomb damping is present in connections or joints where interfacial rubbing dissipates energy. The resulting damping force is nearly constant. It is expressed as: $F_D = \mu N$; where μ is the kinetic friction coefficient; and N is the normal pressure force. Coulomb damping is ignored in the present analysis since it is assumed that the elastic members (i.e., booms, solar arrays, etc.) of the space station are uniform and free of interconnections.

Damping is considered to be rate-dependent (i.e., it depends on the rate of a cyclic load amplitude and on the rate of the deflections). Damping can be incorporated into a vibratory system by specifying a value of the damping factor ζ. The use of viscous damping can be used when the material exhibits nearly elastic behavior. This usually occurs at low amplitudes of stress. For most spacecraft applications, viscous damping can be assumed since deformations are usually small.

In the field of vibrational analysis, it is general knowledge that for lightly damped structures the natural frequencies and mode shapes are largely independent of damping. The motion of an elastic body analyzed under the assumptions of model analyses can be found without considering the specific nature of the dissipation mechanism.

Furthermore, the mode shapes of the elastic appendages can be described accurately for all tumbling spacecraft using only the first

few modes. These lower mode shapes will dominate the response of spacecraft motion.

Observations show that the energy per cycle removed by structural friction is roughly proportional to the square of the amplitude by independent of frequency.[5] This fact demonstrates a significant difference from the simpler case of viscous friction. Consider a simple periodic motion $c = x_o \sin \omega t$ which is opposed by a viscous damping force $F_{D.V.} = -Cx = - c\omega x_o \cos \omega t = \pm c\omega\sqrt{x_o^2 - x^2}$ where the sign is determined from the fact that $F_{D.V.}$ is always opposite to the instantaneous velocity. The work per cycle,

$$W_{D.V.} = \int_{t=0}^{t=2\pi/\omega} F_{D.V.}\, dx,$$

done by $F_{D.V.}$ on the vibrational motion is the area inside the ellipse. Since this diagram would have semiaxes $c\omega x_o$ and x_o, the work per cycle is proportional both to x_o^2 and to ω.

By contrast, a damping force which has the same effect as structural friction would be

$$F_{D.V.} = - gx_o \cos \omega t = \pm g\sqrt{x_o^2 - x^2}\ .$$

The work is again the area inside an ellipse, but the semiaxes are gx_o and x_o. When encountered in cyclic motion of materials, such a force is called hystersis. If one uses the complex representation of simple harmonic motion, $F_{D.S.}$ bags the position vector by 90° and is therefore given by $- igx$, where g is a small structural damping coefficient. One might consider that structural damping is proportional in magnitude to the elastic restoring forces F_E and opposite in direction to the velocity of oscillation.

All representations of structural friction are empirical. The primary purpose is that they provide a means of energy removal that is correctly dependent on the amplitude and frequency.[5,6]

Energy dissipation is modelled as a complex damping term in the equations derived in this appendix. This type of damping has yet to be proven satisfactory for this study.

III. A SPACE STATION WITH FLEXIBLE BEAMS

An investigation of a tumbling space station with long, flexible booms is presented in this Section. Equations of motion are presented for two particular configurations of space stations.

The two most complex configurations that can be reasonably analyzed by the hybrid-coordinate formulation are examined in this Section. The first configuration is composed of an asymmetric rigid central body and six beams of identical material and circular cross-section as shown in Figure 1. The body axes are OXYZ and the origin is at the center of mass of the satellite. Since the deformations of the beams are assumed small ($\sim$ 10% of their length), the center of mass is assumed fixed. In this space station configuration, the three body axes are always parallel to a line tangent to the root of the antennas. The axis OZ is the axis of greatest moment of inertia; moreover $I_z > I_y > I_x$ will be assumed.

The equations of motion will be derived using variational principles of mechanics. It will be assumed that the orbital motion of the satellite mass center is independent of the orientation of the body. The kinetic energy is given by: $T = \frac{1}{2} \int_m \vec{V} \cdot \vec{V} \, dm$

where V is the velocity of a mass point dm. The kinetic energy expression of a tumbling spacecraft becomes:

$$T = \frac{1}{2} A \omega_x^2 + \frac{1}{2} B \omega_y^2 + \frac{1}{2} C \omega_z^2 - D \omega_y \omega_z \qquad (1)$$

$$- E \omega_x \omega_z - F \omega_x \omega_y + \frac{1}{2} \int_M \dot{u} \cdot \dot{u} \, dm + \omega_x \Gamma_x$$

$$+ \omega_y \Gamma_y + \omega_z \Gamma_z$$

are components of the instantaneous moment of inertia tensor (calculated with respect to the OXYZ axes). The quantity u is the deformation referenced from the underformed state, M is the total mass of the body, and Γ_x, Γ_y, and Γ_z are components of angular momentum due to deformation of the configuration. The total angular momentum which remains constant throughout the analysis is

$$h = I \cdot \omega + \Gamma \qquad (2)$$

where I is the inertia tensor of the deformed body and

$$\Gamma \equiv \int_m (r \times u) \, dm$$

is the angular momentum of deformation.

The mechanics of deformation of flexible appendages is first examined. Consider a single beam along OX axis in the undeformed state. Assume the beam is subject to small deflections in the y - and z - direction. The moments and products of inertia are defined as:

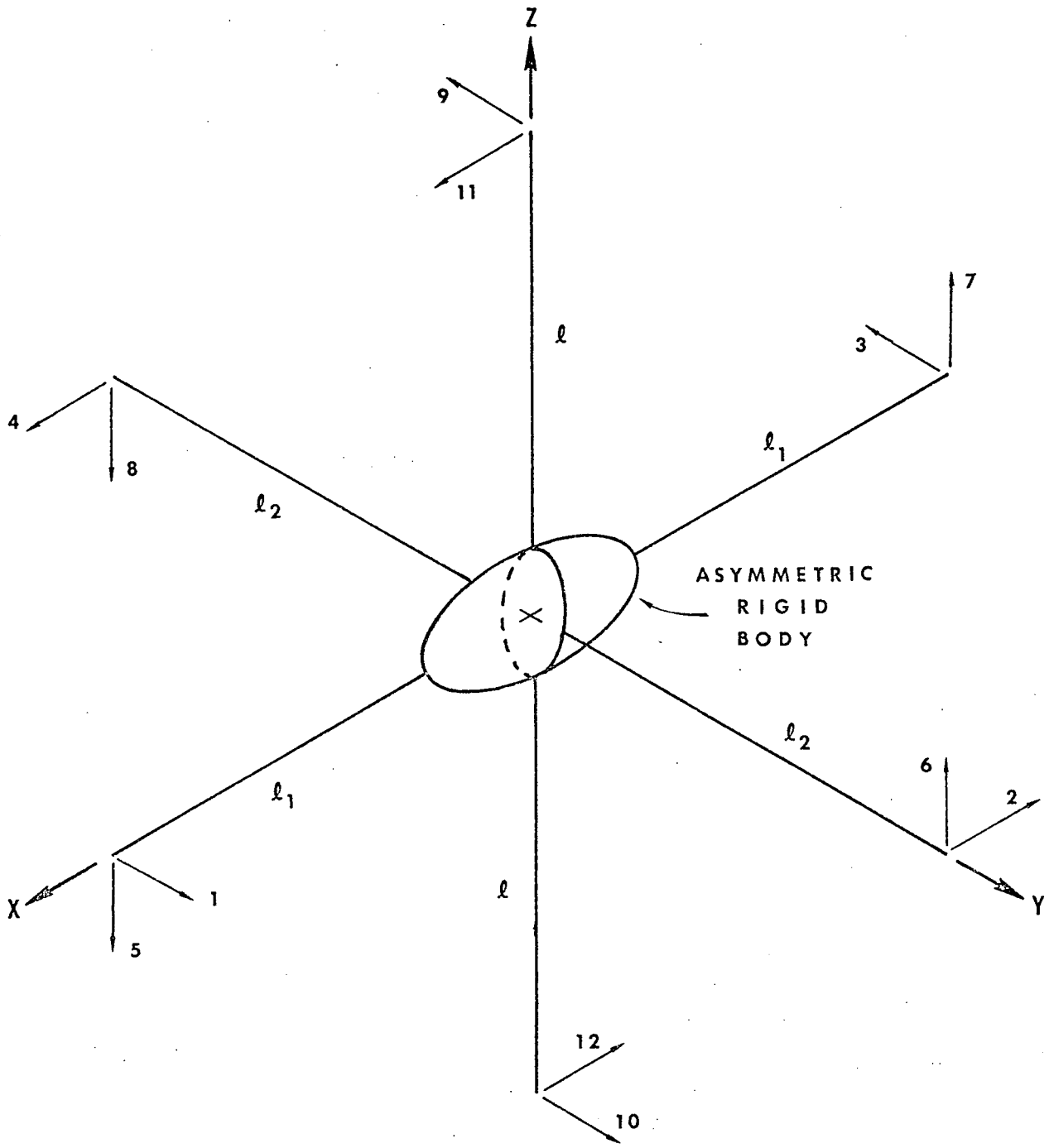

Figure 1. Space Station with Six Flexible Beams.

$$I_x = \int_m (z^2 + y^2)\, dm; \qquad I_{xy} = \int_m xy\, dm$$

$$I_y = \int_m (x^2 + z^2)\, dm; \qquad I_{yz} = \int_m yz\, dm$$

$$I_z = \int_m (y^2 + x^2)\, dm; \qquad I_{xz} = \int_m xz\, dm$$

where m is the total mass of the beam. The beam of length ℓ will shorten upon deformation, and will project a length OX_1 along OX axes (See Figure 2) given by:

$$x_1 = \ell - \frac{1}{2} \int_o^1 \{(\frac{dy}{dx})^2 + (\frac{dz}{dx})^2\}\, dx + H.O.T. \tag{4}$$

The component, C, is expressed as

$$C = \rho \int_o^{\ell} (x^2 + y^2)\, ds \tag{5}$$

where ρ is the mass per unit length and ds is the differential element of arc length. The expression for C can be written as:

$$C = \rho \int_o^{x_1} (x^2 + y^2)\, [1 + \frac{1}{2} (y')^2 + \frac{1}{2} (z')^2 + H.O.T.]\, dx \tag{6}$$

where

$$ds = [1 + (y')^2 + (Z')^2]^{1/2}\, dx = [1 + \frac{1}{2} (y')^2 + \frac{1}{2} (z')^2 + H.O.T.]\, dx$$

has been substituted.

Upon integration C becomes:

$$C = \rho \frac{\ell^3}{3} + \rho \int_o^{\ell} \{y^2 - (\frac{\ell^2 - x^2}{2})\, [(y')^2 + (Z')^2]\}\, dx + H.O.T. \tag{7}$$

where the primes denote differentiation with respect to x.

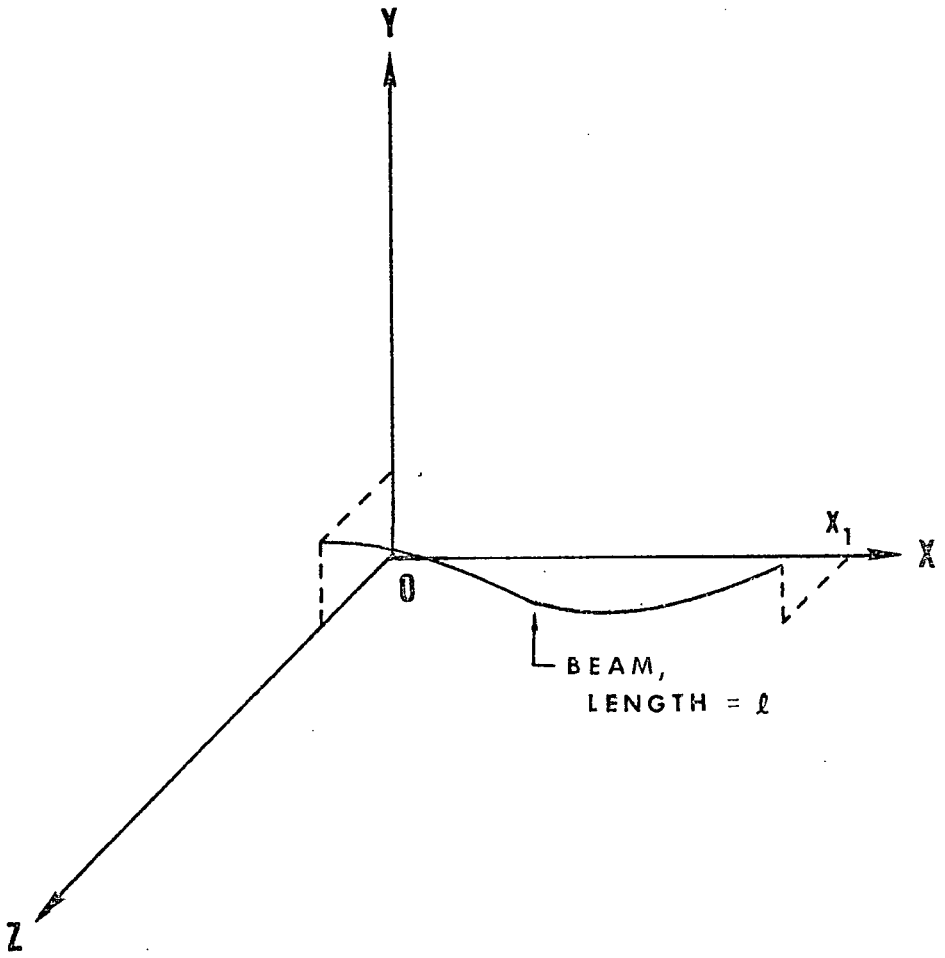

$$X_1 = \ell - \frac{1}{2}\int_0^1 \left[(y')^2 + (z')^2\right] dx + \text{H.O.T.}$$

Figure 2. Single Beam in Deformed State

In a similar manner, the other components of the inertia tensor can be computed. The remaining expressions in the kinetic energy aan be found.[7]

In each case, the body axis XYZ are assumed parallel to the principal axes of the central body and to have an angular velocity $\omega = (\omega_x, \omega_y, \omega_z)$. The first configuration has six beams and there has been defined twelve deformations, $w^i(x,t)$, i - (1,...12) (see Figure 1).

The deformation functions are from modal analysis and are given by:

$$w^i = \sum_{n=1}^{\infty} \ell_i \, q_{in}(t) \, \phi_{in}(\zeta) \tag{8}$$

where $q_{in}(t)$ is a dimensionless coordinate function of the ith beam $\ell_i \, \phi_{in}(\zeta)$ are the normal mode shapes functions. Normally, the procedure is to use the cantilever modes of vibration as computed from the cantilever beam equation:

$$\phi_n''''(\zeta) - \frac{f_{in}^2 \, \rho \, \ell_i^4}{EI} \phi_n(\zeta) = 0 \tag{9}$$

with $\phi_n(0) = \phi_n(1) = \phi_n''(1) = \phi_n'''(1) = 0$.

It is assumed that only the first mode shape will be excited. Higher mode shapes corresponding to higher frequencies will be assumed to have a negligible contribution in this analysis. It is therefore more practical to use an approximate expression for the first cantilever beam mode shape:

$$\phi_1(\zeta) = 1 - \cos \frac{\pi}{2} \zeta \qquad \text{where } \zeta = \frac{x_i}{\ell_i}$$

Greater refinements can be made, however, mathematical complications will result. Certain corrections due to centrifugal stiffening effects may be included, but such effects are negligible for first mode approximations and intermediate values of angular velocities.[8] The decoupling of this problem through the use of antisymmetric and symmetric modes of deformation is not considered. No decoupling techniques are used in this analysis. The only assumption concerning the effect of the deflections on the total vehicle is that the center of mass of the configuration remain fixed. This assumption will be satisfied if the weight ratio of the long, flexible beams to the rigid central body is very small (i.e., on the order of 1:100).

Previously, the geneal kinetic energy expression was written. The potential energy of the system is that due to strain energy of the beams, i.e.,

$$U = \sum_{i=1}^{12} \frac{1}{2} EI \int_{o}^{\ell} \left(\frac{\partial^2 w_i}{\partial x^2}\right)^2 dx \qquad (10)$$

Gravitational potential energy is not included.

It is assumed that damping of each beam will be modelled as structural damping given by complex notation:

$$F_{D.S.} = F_{E.R.} (1 + ig) \qquad (11)$$

where

$F_{E.R.} = \frac{\partial U}{\partial q_{in}}$ which are the elastic restoring forces in the equations of motion.

g = damping factor

$i = \sqrt{-1}$

The equations of motion will be obtained from Lagrange's equations, using the sets $(\omega_x,\omega_y,\omega_z)$ and (q_{in}) as generalized coordinates.

The coordinates ω_x, ω_y, ω_z are quasi-coordinates. The Lagrange's equations are:

$$\frac{d}{dt}\left(\frac{\partial T}{\partial \omega_x}\right) - \omega_z \frac{\partial T}{\partial \omega_y} + \omega_y \frac{\partial T}{\partial \omega_z} = N_x \quad (12a)$$

$$\frac{d}{dt}\left(\frac{\partial T}{\partial \omega_y}\right) - \omega_x \frac{\partial T}{\partial \omega_z} + \omega_z \frac{\partial T}{\partial \omega_x} = N_y \quad (12b)$$

$$\frac{d}{dt}\left(\frac{\partial T}{\partial \omega_z}\right) - \omega_y \frac{\partial T}{\partial \omega_x} + \omega_x \frac{\partial T}{\partial \omega_y} = N_z \quad (12c)$$

where N_x, N_y, N_z are externally applied torques about the XYZ axes. Assuming an uncontrollable tumbling body and no environmental torques; N_x, N_y, N_z are zero.

Substitution of the kinetic energy expression into the Lagrange's equations results in:

$$\frac{d}{dt}\left[I_x\omega_x - I_{xy}\omega_y - I_{xz}\omega_z + \Gamma_x\right] + (I_z - I_y)\omega_y\omega_z + I_{yz}(\omega_z^2 - \omega_y^2) + I_{xy}\omega_x\omega_z - I_{xz}\omega_x\omega_y + \omega_y\Gamma_z - \omega_z\Gamma_y = N_x \quad (13)$$

$$\frac{d}{dt}\left[I_y\omega_y - I_{yz}\omega_z - I_{xy}\omega_x + \Gamma_y\right] + (I_x - I_z)\omega_z\omega_x + I_{xz}(\omega_x^2 - \omega_z^2) + I_{yz}\omega_y\omega_x - I_{xy}\omega_y\omega_z + \omega_z\Gamma_x - \omega_x\Gamma_z = N_y$$

$$\frac{d}{dt}\left[I_z\omega_z - I_{xz}\omega_x - I_{yz}\omega_y + \Gamma_z\right] + (I_y - I_x)\omega_x\omega_y + I_{xy}\cdot$$

$$(\omega_y^2 - \omega_x^2) + I_{xz}\,\omega_z\,\omega_y - I_{yz}\,\omega_z\,\omega_x + \omega_x\Gamma_y - \omega_y\Gamma_x = N_z$$

The expressions for the moments and products of inertia in terms of generalized coordinates are:

$$I_x = I_x' + \mu\ell_2^3\left[N_1(q_{61}^2 + q_{81}^2) - \varepsilon_{11}(q_{21}q_{21} + q_{41}q_{41} + q_{61}q_{61} + q_{81}q_{81})\right] + \mu\ell^3\left[N_1(q_{91}^2 + q_{(10)1}^2) - \varepsilon_{11}(q_{91}q_{91} + q_{(11)1}q_{(11)1} + q_{(10)1}q_{(10)1} + q_{(12)1}q_{(12)1})\right] + \mu\ell_1^3 N_1(q_{11}^2 + q_{51}^2 + q_{51}^2 + q_{71}^2) \tag{14a}$$

$$I_y = I_y' + \mu\ell_1^3\left[N_1(q_{51}^2 + q_{71}^2) - \varepsilon_{11}(q_{11}q_{11} + q_{31}q_{31} + q_{51}q_{51} + q_{71}q_{71})\right] + \mu\ell^3\left[N_1(q_{(11)1}^2 + q_{(12)1}^2) - \varepsilon_{11}(q_{91}q_{91} + q_{(11)1}q_{(11)1} + q_{(12)1}q_{(12)1} + q_{(10)1}q_{(10)1})\right] + \mu\ell_2^3 N_1(q_{61}^2 + q_{21}^2 + q_{41}^2 + q_{81}^2) \tag{14b}$$

$$I_z = I_z' + \mu\ell_1^3\left[N_1(q_{11}^2 + q_{31}^2) - \varepsilon_{11}(q_{11}q_{11} + q_{31}q_{31} + q_{51}q_{51} + q_{71}q_{71})\right] + \mu\ell_2^3\left[N_1(q_{21}^2 + q_{41}^2) - \varepsilon_{11}(q_{21}q_{21} + q_{41}q_{41} + q_{61}q_{61} + q_{81}q_{81})\right] + \mu\ell^3 N_1(q_{91}^2 + q_{(11)1}^2 + q_{(12)1}^2 + q_{(10)1}^2) \tag{14c}$$

$$I_{xy} = \mu\ell_1^3 P_1(q_{11} + q_{31}) - \mu\ell_2^3 P_1(q_{21} + q_{41}) - \mu\ell^3 N_1(q_{91}q_{(11)1} + q_{(10)1}q_{(12)1}) \tag{14d}$$

$$I_{xz} = \mu \ell^3 P_1 (q_{(11),1} + q_{(12),1}) - \mu \ell_1^3 P_1 (q_{5,1} + q_{7,1}) - \mu \ell_2^3 N_1 (q_{2,1} q_{6,1} + q_{4,1} q_{8,1}) \quad (14e)$$

$$I_{yz} = \mu \ell_2^3 P_1 (q_{6,1} + q_{8,1}) - \mu \ell^3 P_1 (q_{9,1} + q_{(10),1}) - \mu \ell_1^3 N_1 (q_{1,1} q_{5,1} + q_{3,1} q_{7,1}) \quad (14f)$$

where I_x', I_y', I_2' are the moments of inertia of the undeformed spacecraft.

$$\delta_{11} N_1 = \int_0^1 \phi_1^2 (\zeta)\, d\zeta$$

$$\varepsilon_{11} = \int_0^1 \left(\frac{1 - \zeta^2}{2}\right) \phi_1''(\zeta)\, \phi_1'(\zeta)\, d\zeta$$

$$p = \int_0^1 \zeta\, \phi_1 (\zeta)\, d\zeta$$

The components of Γ_x, Γ_y, Γ_z become:

$$\Gamma_x = \mu \ell_2^3 P_1 (\dot{q}_{6,1} + \dot{q}_{8,1}) + \mu \ell^3 P_1 (\dot{q}_{9,1} + \dot{q}_{(10),1}) + \mu \ell_1^3 N_1 (\dot{q}_{1,1} q_{5,1} - \dot{q}_{5,1} q_{1,1} + \dot{q}_{3,1} q_{7,1} - \dot{q}_{7,1} q_{3,1}) \quad (15a)$$

$$\Gamma_y = \mu \ell_1^3 P_1 (\dot{q}_{5,1} + \dot{q}_{7,1}) + \mu \ell^3 P_1 (\dot{q}_{(11),1} + \dot{q}_{(12),1}) + \mu \ell_2^3 N_1 (\dot{q}_{2,1} q_{6,1} - q_{2,1} \dot{q}_{6,1} + \dot{q}_{4,1} q_{8,1} - q_{4,1} \dot{q}_{8,1}) \quad (15b)$$

$$\Gamma_2 = \mu l_1^3 P_1 (\dot{q}_{11} + \dot{q}_{31}) + \mu l_2^3 P_1 (\dot{q}_{21} + \dot{q}_{91}) + \mu l^3 N_1 (\dot{q}_{91} q_{(11)1} - q_{91} \dot{q}_{(11)1} + \dot{q}_{(10)1} q_{(12)1} - q_{(10)1} \dot{q}_{(12)1}) \quad (15c)$$

The Lagrange's equations of motion for the appendages are:

$$\frac{d}{dt} \left(\frac{\partial L}{\partial \dot{q}_{in}}\right) - \frac{\partial L}{\partial q_{in}} = 0$$

where

$$L = T - U$$

q_{il} = generalized coordinate for n = 1 (first mode and i = 1,...12

The expression for the potential energy is:

$$U = \frac{1}{2} \mu l_1^3 f_{11}^2 N_1 (q_{11}^2 + q_{31}^2 + q_{51}^2 + q_{71}^2) + 1/2 \mu l_2^3 f_{21}^2 N_1 (q_{21}^2 + q_{41}^2 + q_{61}^2 + q_{81}^2) + \frac{1}{2} \mu l^3 f_{l1}^2 N_1 (q_{91}^2 + q_{(10)1}^2 + q_{(11)1}^2 + q_{(12)1}^2) \quad (16)$$

where f_{il} ≡ natural frequency of the ith beam. The deformation term is:

$$\frac{1}{2} \int_m \dot{u} \cdot \dot{u} \, dm = \frac{1}{2} \mu l_1^3 N_1 (\dot{q}_{11}^2 + \dot{q}_{51}^2 + \dot{q}_{31}^2 + \dot{q}_{71}^2) + \frac{1}{2} \mu l_2^3 N_1 (\dot{q}_{21}^2 + \dot{q}_{61}^2 + \dot{q}_{41}^2 + \dot{q}_{81}^2) + \frac{1}{2} \mu l^3 N_1 (\dot{q}_{91}^2 + \dot{q}_{(10)1}^2 + \dot{q}_{(11)1}^2 + \dot{q}_{(12)1}^2) \quad (17)$$

Knowing these expressions, the twelve equations of motion for the flexible appendages can be written:

$$\ddot{q}_{11} + (1+ig) f_{11}^2 q_{11} + \left[\left(\frac{\varepsilon_{11}}{\Delta V_1} - 1\right)\omega_z^2 - \omega_x^2 + \frac{\varepsilon_{11}}{\Delta V_1}\omega_y^2\right] q_{11} + 2\omega_x \dot{q}_{51} + (\dot{\omega}_x - \omega_y\omega_z) q_{51} + \frac{\rho_1}{\Delta V_1}(\dot{\omega}_z + \omega_x\omega_y) = 0 \tag{18a}$$

$$\ddot{q}_{21} + (1+ig) f_{21}^2 q_{21} + \left[\left(\frac{\varepsilon_{11}}{\Delta V_1} - 1\right)\omega_z^2 - \omega_y^2 + \frac{\varepsilon_{11}}{\Delta V_1}\omega_x^2\right] q_{21} - 2\omega_y \dot{q}_{61} - (\dot{\omega}_y - \omega_x\omega_z) q_{61} + \frac{\rho_1}{\Delta V_1}(\dot{\omega}_z - \omega_x\omega_y) = 0 \tag{18b}$$

$$\ddot{q}_{31} + (1+ig) f_{11}^2 q_{31} + \left[\left(\frac{\varepsilon_{11}}{\Delta V_1} - 1\right)\omega_z^2 - \omega_x^2 + \frac{\varepsilon_{11}}{\Delta V_1}\omega_y^2\right] q_{31} + 2\omega_x \dot{q}_{71} + (\dot{\omega}_x - \omega_y\omega_z) q_{71} + \frac{\rho_1}{\Delta V_1}(\dot{\omega}_z + \omega_x\omega_y) = 0 \tag{18c}$$

$$\ddot{q}_{41} + (1+ig) f_{21}^2 q_{41} + \left[\left(\frac{\varepsilon_{11}}{\Delta V_1} - 1\right)\omega_z^2 - \omega_y^2 + \frac{\varepsilon_{11}}{\Delta V_1}\omega_x^2\right] q_{41} - 2\omega_y \dot{q}_{81} - (\dot{\omega}_y - \omega_x\omega_z) q_{81} + \frac{\rho_1}{\Delta V_1}(\dot{\omega}_z - \omega_x\omega_y) = 0 \tag{18d}$$

$$\ddot{q}_{51} + (1+ig) f_{11}^2 q_{51} + \left[\left(\frac{\varepsilon_{11}}{\Delta V_1} - 1\right)\omega_y^2 - \omega_x^2 + \frac{\varepsilon_{11}}{\Delta V_1}\omega_z^2\right] q_{51} - 2\omega_x \dot{q}_{11} - (\dot{\omega}_x + \omega_y\omega_z) q_{11} + \frac{\rho_1}{\Delta V_1}(\dot{\omega}_y - \omega_x\omega_z) = 0 \tag{18e}$$

$$\ddot{q}_{61} + (1+ig) f_{21}^2 q_{61} + \left[\left(\frac{\varepsilon_{11}}{\Delta I_1} - 1 \right) \omega_x^2 - \omega_y^2 + \frac{\varepsilon_{11}}{\Delta I_1} \omega_z^2 \right] q_{61} + 2\omega_y \dot{q}_{21} + (\dot{\omega}_y - \omega_x \omega_z) q_{21} + \frac{\rho_1}{\Delta I_1} (\dot{\omega}_x + \omega_y \omega_z) = 0 \tag{18f}$$

$$\ddot{q}_{71} + (1+ig) f_{11}^2 q_{71} + \left[\left(\frac{\varepsilon_{11}}{\Delta I_1} - 1 \right) \omega_y^2 - \omega_x^2 + \frac{\varepsilon_{11}}{\Delta I_1} \omega_z^2 \right] q_{71} - 2\omega_x \dot{q}_{31} - (\dot{\omega}_x + \omega_y \omega_z) q_{31} + \frac{\rho_1}{\Delta I_1} (\dot{\omega}_y - \omega_x \omega_z) = 0 \tag{18g}$$

$$\ddot{q}_{81} + (1+ig) f_{21}^2 q_{81} + \left[\left(\frac{\varepsilon_{11}}{\Delta I_1} - 1 \right) \omega_x^2 - \omega_y^2 + \frac{\varepsilon_{11}}{\Delta I_1} \omega_z^2 \right] q_{81} + 2\omega_y \dot{q}_{91} + (\dot{\omega}_y - \omega_x \omega_z) q_{91} + \frac{\rho_1}{\Delta I_1} (\dot{\omega}_x + \omega_y \omega_z) = 0 \tag{18h}$$

$$\ddot{q}_{91} + (1+ig) f_{21}^2 q_{91} + \left[\left(\frac{\varepsilon_{11}}{\Delta I_1} - 1 \right) \omega_x^2 - \omega_z^2 + \frac{\varepsilon_{11}}{\Delta I_1} \omega_y^2 \right] q_{91} + 2\omega_z \dot{q}_{(11)1} + (\dot{\omega}_z - \omega_x \omega_y) q_{(11)1} + \frac{\rho_1}{\Delta I_1} (\dot{\omega}_x - \omega_y \omega_z) = 0 \tag{18i}$$

$$\ddot{q}_{(10)1} + (1+ig) f_{21}^2 q_{(10)1} + \left[\left(\frac{\varepsilon_{11}}{\Delta I_1} - 1 \right) \omega_x^2 - \omega_z^2 + \frac{\varepsilon_{11}}{\Delta I_1} \omega_y^2 \right] q_{(10)1} + 2\omega_z \dot{q}_{(12)1} + (\dot{\omega}_z - \omega_x \omega_y) q_{(12)1} + \frac{\rho_1}{\Delta I_1} (\dot{\omega}_x - \omega_y \omega_z) = 0 \tag{18j}$$

$$\ddot{q}_{(11)_1} + (1+ig) f_{e_1}^2 q_{(11)_1} + \left[\left(\frac{\varepsilon_{11}}{\Delta T_1} - 1 \right) \omega_y^2 - \omega_z^2 + \frac{\varepsilon_{11}}{\Delta T_1} \omega_x^2 \right] q_{(11)_1} - 2\omega_z \dot{q}_{q1} - (\dot{\omega}_z + \omega_x \omega_y) q_{q1} + \frac{\rho_1}{\Delta T_1} (\dot{\omega}_y + \omega_x \omega_z) = 0 \tag{18k}$$

$$\ddot{q}_{(12)_1} + (1+ig) f_{e_1}^2 q_{(12)_1} + \left[\left(\frac{\varepsilon_{11}}{\Delta T_1} - 1 \right) \omega_y^2 - \omega_z^2 + \frac{\varepsilon_{11}}{\Delta T_1} \omega_x^2 \right] q_{(12)_1} - 2\omega_z \dot{q}_{(10)_1} - (\dot{\omega}_z + \omega_x \omega_y) q_{(10)_1} + \frac{\rho_1}{\Delta T_1} (\dot{\omega}_y + \omega_x \omega_z) = 0 \tag{181}$$

Equations (13), together with Equations (14), (15), and (18) are the motion equations for the space station. They will be integrated numerically by digital computer under the assumption n = 1.

It must be stressed that the equations are valid only for small deflection of the beams. The angular velocities (ω_x,ω_y,ω_z) need not be small.

In the equations of motion for the appendages the damping factor has been included.

In the last section of this report, there is a brief discussion on the values of the constants and initial conditions that will be used to initiate the solutions to these equations.

The next configuration of space craft to be considered is shown in Figure 2. In this case, one of the radial appendages has been removed and the remaining three are placed symmetrically about the z-axis. The angle γ is used to designate the angle between two successive appendages and is found by dividing 360° by the number of appendages in x-y plane (in this case N = 3).

The development of the equations of motion for this configuration follows the same procedure as used for configuration I. The moments and products of inertia about each beam must be found about new axes through and perpendicular to the beam and then rotated through the angle γ. These moments and products of inertia must then be substituted into the following transformation equations:

$$I_{x_1} = I_x \alpha_{11}^2 + I_y \alpha_{21}^2 + I_z \alpha_{31}^2 - 2I_{xy} \alpha_{11} \alpha_{21} - \quad (19a)$$

$$2I_{xz} \alpha_{11} \alpha_{31} - 2I_{yz} \alpha_{21} \alpha_{31}$$

$$I_{y_1} = I_x \alpha_{12}^2 + I_y \alpha_{22}^2 + I_z \alpha_{23}^2 - 2I_{xy} \alpha_{12} \alpha_{22} - \quad (19b)$$

$$2I_{xz} \alpha_{12} \alpha_{32} - 2I_{yz} \alpha_{22} \alpha_{32}$$

$$I_{z_1} = I_x \alpha_{13}^2 + I_y \alpha_{23}^2 + I_z \alpha_{33}^2 - 2I_{xy} \alpha_{13} \alpha_{23} - \quad (19c)$$

$$2I_{xz} \alpha_{13} \alpha_{33} - 2I_{yz} \alpha_{23} \alpha_{33}$$

$$I_{x_1 y_1} = (\alpha_{11} \alpha_{22} + \alpha_{12} \alpha_{21}) I_{xy} + (\alpha_{11} \alpha_{32} + \alpha_{12} \alpha_{31}) I_{xz} \quad (19d)$$

$$+ (\alpha_{21} \alpha_{32} + \alpha_{22} \alpha_{31}) I_{yz} - (\alpha_{11} \alpha_{12} I_x + \alpha_{21} \alpha_{22}$$

$$I_y + \alpha_{31} \alpha_{32} I_z)$$

$$I_{x_1 z_1} = (\alpha_{11} \alpha_{32} + \alpha_{12} \alpha_{31}) I_{xy} + (\alpha_{11} \alpha_{33} + \alpha_{13} \alpha_{31}) \quad (19e)$$

$$I_{xz} + (\alpha_{12} \alpha_{33} + \alpha_{32} \alpha_{13}) I_{yz} - (\alpha_{11} \alpha_{31} I_x +$$

$$\alpha_{12} \alpha_{32} I_y + \alpha_{13} \alpha_{33} I_z)$$

$$I_{y_1 z_1} = (\alpha_{21} \alpha_{32} + \alpha_{22} \alpha_{31}) I_{xy} + (\alpha_{21} \alpha_{33} + \alpha_{31} \alpha_{23}) \quad (19f)$$

$$I_{xz} + (\alpha_{22} \alpha_{33} + \alpha_{23} \alpha_{32}) I_{yz} - (\alpha_{21} \alpha_{31} I_x +$$

$$\alpha_{22} \alpha_{32} I_y + \alpha_{23} \alpha_{33} I_z)$$

$$I_x = I_x' + \frac{1}{4}\left[\mu l_1^3 N_1 (q_{11}^2 + q_{41}^2) + \mu l_2^3 N_1 (q_{21}^2 + q_{51}^2) + \mu l_3^3 N_1 (q_{31}^2 + q_{61}^2)\right] + \frac{3}{4}\left[\mu l_1^3 (N_1 q_{41}^2 - \varepsilon_{11}(q_{11}q_{11} + q_{41}q_{41})) + \mu l_2^3 (N_1 q_{51}^2 - \varepsilon_{11}(q_{21}q_{21} + q_{51}q_{51})) + \mu l_3^3 (N_1 q_{61}^2 - \varepsilon_{11}(q_{31}q_{31} + q_{61}q_{61}))\right] + \frac{1}{2}\sqrt{3}\left[\mu l_1^3 f_1 q_{11} + \mu l_2^3 f_1 q_{21} + \mu l_3^3 f_1 q_{31}\right] + \mu l^3 \left[N_1 (q_{71}^2 + q_{81}^2) - \varepsilon_{11}(q_{71}q_{71} + q_{81}q_{81} + q_{91}q_{91} + q_{(10)1}q_{(10)1})\right] \quad (20a)$$

$$I_y = I_y' + \frac{3}{4}\left[\mu l_1^3 N_1 (q_{11}^2 + q_{41}^2) + \mu l_2^3 N_1 (q_{21}^2 + q_{51}^2) + \mu l_3^3 N_1 (q_{31}^2 + q_{61}^2)\right] + \frac{3}{4}\left[\mu l_1^3 (N_1 q_{41}^2 - \varepsilon_{11}(q_{11}q_{11} + q_{41}q_{41})) + \mu l_2^3 (N_1 q_{51}^2 - \varepsilon_{11}(q_{21}q_{21} + q_{51}q_{51})) + \mu l_3^3 (N_1 q_{61}^2 - \varepsilon_{11}(q_{31}q_{31} + q_{61}q_{61}))\right] + \frac{3}{2}\left[\mu l_1^3 f_1 q_{11} + \mu l_2^3 f_1 q_{21} + \mu l_3^3 f_1 q_{31}\right] + \mu l^3 \left[N_1 (q_{71}^2 + q_{81}^2 + q_{91}^2 + q_{(10)1}^2) - \varepsilon_{11}(q_{71}q_{71} + q_{81}q_{81} + q_{91}q_{91} + q_{(10)1}q_{(10)1})\right] \quad (20b)$$

$$I_z = I_z' + \mu l_1^3 \left[N_1 q_{11}^2 - \varepsilon_{11}(q_{11}q_{11} + q_{41}q_{41})\right] + \mu l_2^3 \left[N_1 q_{21}^2 - \varepsilon_{11}(q_{21}q_{21} + q_{51}q_{51})\right] + \mu l_3^3 \left[N_1 q_{31}^2 - \varepsilon_{11}(q_{31}q_{31} + q_{61}q_{61})\right] + \mu l^3 N_1 (q_{71}^2 + q_{91}^2 + q_{81}^2 + q_{(10)1}^2) \quad (20c)$$

where α_{ij} are direction cosines of axis i with respect to axis j.

The direction cosines for this problem are:

$\alpha_{11} = \cos \gamma$, $\alpha_{22} = -\sin \gamma$, $\alpha_{12} = \alpha_{21} = \sin \gamma$, and $\alpha_{31} = \alpha_{23} = 0$.

This means for $\alpha = 120°$, $\alpha_{11} = -5$, $\alpha_{22} = -.866$, $\alpha_{21} = \alpha_{12} = .866$.

The moments and products of inertias may be written:

$$I_x = \frac{1}{4} (I_{x_{1,2,3}}) + \frac{3}{4} (I_{y_{1,2,3}}) + .866 (I_{xy_{1,2,3}})$$

$$I_y = \frac{3}{4} (I_{x_{1,2,3}}) + \frac{3}{4} (I_{y_{1,2,3}}) + \frac{3}{2} (I_{xy_{1,2,3}})$$

I_z = remains the same as before as the z-axis was not rotated

$$I_{xy} = (\frac{3}{4} + \frac{1}{4}\sqrt{3}) (I_{xy_{1,2,3}}) + \frac{1}{4}\sqrt{3} (I_{x_{1,2,3}}) + \frac{3}{4} (I_{y_{1,2,3}})$$

I_{xz} and I_{yz} do not change.

where $I_{x_{1,2,3}}$ = the moment of inertia about an x-axis through beams 1,2,3

It should be noted that there is one less beam to consider in this configuration and new generalized coordinates are defined for this case (see Figure 3).

The expression for the moments and products of inertia are:

$$I_{xy} = \left(\frac{3}{4} + \frac{1}{4}\sqrt{3}\right)\left[\mu l_1^3 f_1 g_{11} + \mu l_2^3 f_1 g_{21}' + \mu l_3^3 f_1 g_{31}'\right] + \frac{1}{4}\sqrt{3}\left[\mu l_1^3 N_1 (g_{11}^2 + g_{41}^2) + \mu l_2^3 N_1 (g_{21}^2 + g_{51}^2) + \mu l_3^3 N_1 (g_{31}^2 + g_{61}^2)\right] + \frac{3}{4}\left[\mu l_1^3 (N_1 g_{41}^2 - \varepsilon_{11}(g_{11} g_{11} + g_{41} g_{41})) + \mu l_2^3 (N_1 g_{51}^2 - \varepsilon_{11}(g_{21} g_{21} + g_{51} g_{51})) + \mu l_3^3 (N_1 g_{61}^2 - \varepsilon_{11}(g_{31} g_{31} + g_{61} g_{61}))\right] - \mu l^3 N_1 (g_{71} g_{91} + g_{81} g_{(10)1}) \quad (20d)$$

$$I_{xz} = \mu l^3 f_1 (g_{91} + g_{(10)1}) - \mu l_1^3 f_1 g_{41} - \mu l_2^3 N_1 (g_{21}' g_{51}) - \mu l_3^3 N_1 (g_{31}' g_{61}') \quad (20e)$$

$$I_{yz} = \mu l_2^3 f_1 g_{51} - \mu l_1^3 N_1 g_{11} g_{41} + \mu l_3^3 f_1 g_{61} - \mu l^3 f_1 (g_{71} + g_{81}) \quad (20f)$$

where: $g_{21}' = -g_{21} \sin\gamma$

$g_{31}' = -g_{31} \sin\gamma$

Now Γ_{x_1} Γ_{y_1} Γ_z are:

$$\Gamma_x = \mu \ell^3 f_1 (\ddot{q}_{71} + \ddot{q}_{81}) + \mu l_1^3 N_1 (\ddot{q}_{11} q_{91} - \ddot{q}_{41} q_{11}) + \mu l_2^3 \sin^2\gamma_i f_1 \ddot{q}_{51} + \mu l_3^3 \sin^2\gamma_i f_1 \ddot{q}_{61} \quad (21a)$$

$$\Gamma_y = \mu l_1^3 f_1 \ddot{q}_{41} + \mu \ell^3 f_1 (\ddot{q}_{91} + \ddot{q}_{(10)1}) + \mu l_2^3 \sin^2\gamma_i N_1 (\ddot{q}_{21}' q_{51} - q_{21}' \ddot{q}_{51}) + \mu l_3^3 \sin^2\gamma_i N_1 (\ddot{q}_{31}' q_{61} - \ddot{q}_{61} q_{31}') \quad (21b)$$

$$\Gamma_z = \mu l_1^3 f_1 \ddot{q}_{11} + \mu l_2^3 f_1 \ddot{q}_{21} + \mu l_3^3 f_1 \ddot{q}_{31} + \mu \ell^3 N_1 \ddot{q}_{71} \ddot{q}_{91} - \ddot{q}_{91} q_{71} + \ddot{q}_{81} q_{(10)1} - \ddot{q}_{(10)1} q_{81}) \quad (21c)$$

where: $\gamma_i = 120°$

$$q_{21}' = -q_{21} \sin\gamma_i = -\tfrac{1}{2}\sqrt{3}\, q_{21}$$
$$q_{31}' = -q_{31} \sin\gamma_i = -\tfrac{1}{2}\sqrt{3}\, q_{31}$$

The potential energy is:

$$U = \tfrac{1}{2}\mu l_1^3 f_{11} N_1 (q_{11}^2 + q_{41}^2) + \tfrac{1}{2}\mu l_2^3 f_{21}^2 N_1 (q_{21}^2 + q_{51}^2) + \tfrac{1}{2}\mu l_3^3 f_{31}^2 N_1 (q_{31}^2 + q_{61}^2) + \tfrac{1}{2}\mu \ell^3 f_{\ell_1}^2 N_1 (q_{71}^2 + q_{81}^2 + q_{91}^2 + q_{(10)1}^2) \quad (22)$$

$$\tfrac{1}{2}\int_m \dot{u}\cdot\dot{u}\, dm = \tfrac{1}{2}\mu l_1^3 N_1 (\dot{q}_{11}^2 + \dot{q}_{41}^2) + \tfrac{1}{2}\mu l_2^3 N_1 (\dot{q}_{21}^2 + \dot{q}_{51}^2) + \tfrac{1}{2}\mu l_3^3 N_1 (\dot{q}_{31}^2 + \dot{q}_{61}^2) + \tfrac{1}{2}\mu \ell^3 N_1 (\dot{q}_{71}^2 + \dot{q}_{81}^2 + \dot{q}_{91}^2 + \dot{q}_{(10)1}^2) \quad (23)$$

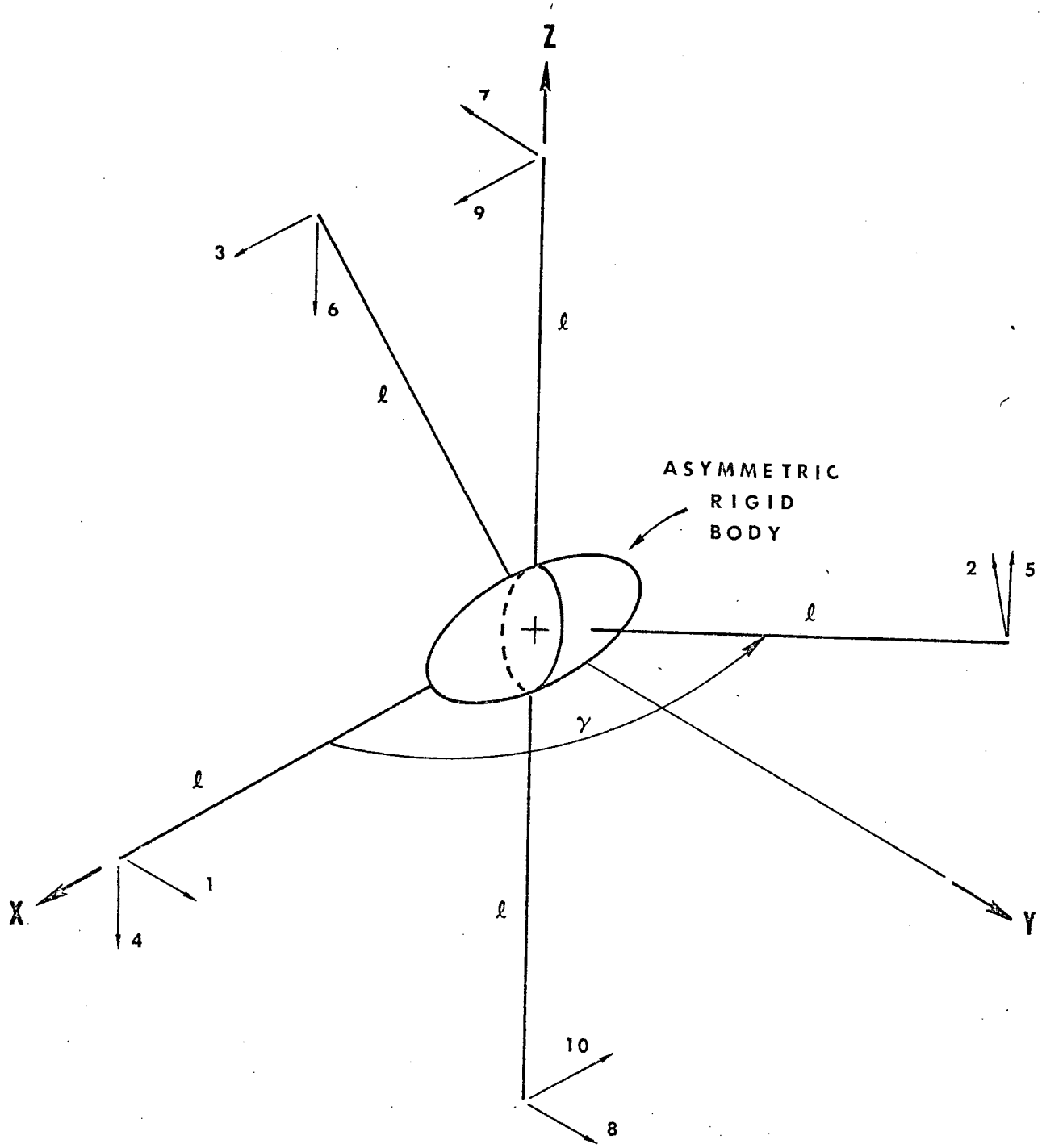

Figure 3. Space Station with Five Flexible Beams

These expressions and substitutions of equations 13 and 18 will result in the equations of motion for configuration II. The same type of structural damping is inserted into these equations as before.

Approaching the problem through a study of just two configurations does not impair the significance of the results. By changing the constants and variables of these configurations a wide range of information should become available.

The technique of obtaining a solution for these configurations consisting of beams is hopefully going to lead to solving the rate of energy dissipation occurring on the tumbling NAR modular space station.

Information is being gathered as to the type of flexible appendages that are attached to the NAR space station. Due to the knowledge gained in analyzing the space stations with beams, the analysis of NAR modular space station with large solar arrays will follow directly.

IV. DISCUSSION OF SIMULATION PARAMETERS

The last Section has shown that the equations of motion for the two configurations of space stations with long, flexible beams contain many constants which must be specified before computer simulation can begin. In this Section, certain initial conditions, parameters, and assumptions for this study which have been decided upon will be presented.

The two configurations of spacecraft are considered to be examples of future space stations whose total mass are 100,000 kg. each (i.e., the same mass as the NAR modular space stations). Each configuration

has an asymmetric, rigid, central body. Energy dissipation comes from the flexure of elastic appendages which differ in number and size from one configuration to the other.

The most important of the parameters are the moments and products of inertia for each vehicle. The asymmetric rigid main body of each configuration will be assumed to have identical moments and products of inertia, that is:

$$I_x(Kg - m^2) = 1.0 \times 10^3$$
$$I_y \quad " \quad = 1.0 \times 10^4$$
$$I_z \quad " \quad = 1.0 \times 10^5$$
$$I_{xy},\ I_{yx},\ I_{xz} = 0$$

Each configuration will have its own moment and products of inertia depending on the number and size of the elastic appendages.

Each space station in this report contains elastic beams. For initial considerations, each beam will have the same length and be constructed from the same material. The booms will be 25 meters long and be constructed of beryllium copper. Beryllium copper is used to construct many antennas on space vehicles and has light-weights and elastic characteristics. Its density (i.e., mass/length) is .00197 Kg/m and its stiffness modulus, EI, is 6.46 $NT\text{-}m^2$.[7] The weight ratio of the main central body with the long appendages is of the order 1:1000. Consequently, it is reasonable to assume that the mass center of the total vehicle does not change position with time during small deformations.

There is still work to be finished on the panel configuration and no decision on the length or material of the panel has been made. Parameters for this structure will be based on the final form of the equations of motion, the method of solution, and the results obtained from computer simulation of configurations I and II.

The most general type of passive attitude motion is considered to be an initial premise to this study. Tumbling motion requires the knowledge of three angular velocities: ω_x, ω_y, and ω_z. Before specifying their numerical values the natureal frequencies of the beams were calculated. With the beams assumed to be uniform and cantilevered, the natural frequencies are found from: $\omega_n = (\beta\ell)^2 \sqrt{EI/m\ell^4}$. The first two natural frequencies are 3.072 cpm and 19.258 cpm. It was decided that only the first mode of vibration should be exicted in this work so the angular velocities were chosen to be a reasonable value of 6.00 rpm each.

The method of solution immediately follows upon knowing the initial angular velocities. For example, in configuration I which has six symmetrically placed beams, the approach to the solution would be as follows: (1) substitute in known parameters (see Table I), (2) set initial conditions, (3) substitute ω_x, ω_y, ω_z into the three satellite equations (4) solve for ω_x, ω_y, ω_z in terms of the q's, (5) substitute ω_x, ω_y, ω_z just found in step (4) into the twelve appendage equations, (6) solve for the q's, (7) knowing the deflections, calculate the values of ω_x, ω_y, ω_z, (8) integrate ω values to get the new ω_x, ω_y, ω_z, (9) repeat process.

TABLE I

$\ell_1 = \ell_2 = \ell_3 = \ldots \ell_6 = 25$ meters	
$\mu = .00197$ Kg/m	
$EI = 6.46$ NT-m^2	
Antenna material - BeCu	
$I_x = 1.0 \times 10^3$ Kg - m^2	
$I_y = 1.0 \times 10^4$	Main Body
$I_z = 1.0 \times 10^5$	
$I_{xy_1}, I_{y_2}, I_{zx} = 0$ Kg - m^2	
$I_x = 1.041 \times 10^3$ Kg - m^2	
$I_y = 1.004 \times 10^4$	Undeformed Total Body
$I_z = 1.0 \times 10^5$	
$I_{xy}, I_{yz}, I_{zx} = 0$ Kg - m^2	
Total Mass = 100,000 Kg	
$M_1 = 1$	
$p_1 = .569$	Integrals in Equations for n = 1
$\varepsilon_{11} = 1.193$	
$f_{in} = 3.072$ cpm	
Initial Conditions:	
$\omega_x = 6.00$ rpm	
$\omega_y = 6.00$ rpm	
$\omega_z = 6.00$ rpm	
$q_{11}, \ldots q_{12}, = 1$	

The stability characteristics of these parameters chosen here will be substantiated or disproved through numerical simulation of the nonlinear equations of motion of the two spacecraft configurations. The presence of an energy dissipation term in the equations will model the damping characteristics of the flexible appendages the rate at which energy is dissipated due to the effects of flexibility will be obtained.

V. REFERENCES FOR APPENDIX D

1. Semi-Annual Progress Report on Dynamics and Control of Escape and Rescue from a Tumbling Spacecraft, NASA Grant NGR 39-009-210, May 1972.

2. Thomson, W. T., Introduction to Space Dynamics, Jphn Wiley & Sons, Inc., New York, 1963.

3. Likins, P. W., "Dynamics and Control of Flexible Space Vehicles," JPL TR 32-1329, Rev. 1, January 15, 1970.

4. Whittaker, E. T., Analytical Dynamics of Particles and Rigid Bodies, Cambridge University Press, 1964.

5. Hurty & Rubenstein, Dynamics of Structures, Prentice-Hall, Inc. Englewood Cuffs, New Jersey, 1964.

6. Bisplinghoff, R. L., Ashley, H., and Halfman, R. L., Aeroelasticity, Addison-Wesley Publishing Co., Inc., Reading, Mass., 1955.

7. Vigneron, F. R., "Stability of a Freely Spinning Satellite of Cross-Dipole Configuration," CASI Transactions, Vol. 3, No. 1, March 1970.

8. Renard, M. and Rakawoski, "A Study of Nutational Behavior of a Flexible Spinning Satellite Using Natural Frequencies and Modes of the Rotating Structures," AIAA Paper No. 70-1046.